Metallic non-Fermi-liquid phases of an extended Hubbard model in infinite dimensions

Qimiao Si and Gabriel Kotliar

Serin Physics Laboratory, Rutgers University, Piscataway, New Jersey 08855-0849

We study an extended Hubbard model in the limit of infinite dimensions and its zero-dimensional counterpart, a generalized asymmetric Anderson model. In the impurity model we find three kinds of mixed valence states: (a) the usual strong-coupling state in which a resonance forms at the Fermi level; (b) a weak-coupling state in which neither the impurity spin nor the impurity charge degrees of freedom are quenched; and (c) an intermediate-coupling state where the spin but not the charge degree of freedom is quenched. The corresponding phases of the extended Hubbard model in infinite dimensions are (a) a Fermi liquid; (b) a non-Fermi-liquid state with incoherent charge and spin excitations; and (c) a non-Fermi-liquid state with incoherent charge but coherent spin excitations. The non-Fermi-liquid phases are incoherent metallic states with vanishing quasiparticle residue, self-similar local correlation functions, and asymptotically decoupled charge and spin excitations. The non-Fermi-liquid phases occur for a wide range of parameters.

I. INTRODUCTION

Various anomalies in the normal state of the high-T_c copper oxides have motivated the current theoretical efforts to search for models that exhibit metallic non-Fermi-liquid states.[1,2] The mechanism for the breakdown of Fermi-liquid theory in one dimension is well understood. For weakly interacting one-dimensional fermion systems, the renormalization group leads to the g-ology classification of spatially homogeneous metallic states. The possible states are Luttinger liquids or those with divergent charge-density wave, spin-density wave, or superconducting correlation functions.[3,4] Bethe ansatz, bosonization, and exact diagonalization methods have been used to show that this classification persists for strong interactions provided that phase separation does not intervene.[5]

In dimensions higher than one, perturbative renormalization-group analysis has shown that, Fermi-liquid theory does describe weakly interacting fermion systems with a regular density of states.[6] Therefore, the mechanism for the breakdown of Fermi-liquid theory is necessarily nonperturbative in the interaction strength. Most of the previous approaches to this problem address under what circumstances the residual interactions between the quasiparticles can acquire singularities. Here we take an alternative approach. We analyze the competition between local correlation and itinerant effects without assuming quasiparticles to begin with. The effect of interactions is treated nonperturbatively. This is carried out in a controlled fashion, by studying this problem in the limit of infinite dimensionality.[7]

In the limit of infinite dimensions, all correlation functions of a lattice fermion model can be reconstructed from the knowledge of the *local* correlators, which can in turn be determined from those of an *associated impurity model*.[8,9] The impurity model describes some local degrees of freedom interacting with a self-consistent electron bath. This limit corresponds to a *dynamical mean-field theory*, within which nontrivial phases can be

studied. The fact that only the low-frequency behavior of the correlators of the bath governs the low-frequency asymptotics of the correlators of the impurity model, suggests that a complete classification of the translationally invariant phases of fermions in the limit of large dimensions could be within reach. The Hubbard model with a Lorentzian density of states maps onto an Anderson model with an *infinite* bandwidth, proving that this model in large dimensions is a Fermi liquid.[8] The Hubbard model in large dimensions with a *bounded* density of states, at half filling and for large U, maps into an Anderson impurity embedded in an insulating medium,[10-12] demonstrating that at large U a frustrated Hubbard model is a Mott insulator. The characterization of the state that results from doping this Mott insulator is still an open problem.

In this paper, we construct and study various metallic non-Fermi-liquid states. These phases are realized in an extended (two-band) Hubbard model, which contains the most general local density-density and spin-spin interactions and a Lorentzian density of states. We stress, however, that the low-energy analysis of the non-Fermi-liquid phases presented here is more general than the particular extended Hubbard model that we studied. We envision that many realistic Hamiltonians will be described, at low energies, by the impurity action that we study in this paper. The spin and charge couplings we discuss will be generated dynamically in the process of renormalization.

The impurity model associated with the extended Hubbard model is a generalized Anderson model. It will be shown that the fact that the impurity model is associated with a lattice model forces the impurity to be near criticality over a range of parameters. Qualitatively, this can be understood very simply in the context of a weakly doped large-U Hubbard model. In this case the correlated site describes the local physics of the one-band Hubbard model and the bath describes the effects of the electrons near that site. The self-consistency condition restores translational invariance and forces the correlated level to be near the chemical potential. In a two-band

model describing a heavy (correlated) level and a light conduction band, the heavy level participates in the charge transport only when it is situated near the chemical potential of the conduction band. The low-energy description of the local physics of the one- and the two-band models is very similar. The role of the light conduction band in the two-band model is played by the incoherent part of the one-particle Green's function in the one-band model.

To study the low-energy behavior of the correlators of the impurity model near the critical point, we set up a renormalization-group (RG) analysis for this problem. Our strategy is to set up an expansion in terms of the hopping amplitudes between the local configurations of the impurity problem. This is an extension of the classic work of Haldane.[13] The resulting expression of the partition function resembles that of a classical Coulomb gas. The hopping amplitudes correspond to fugacities of the Coulomb-gas representation. The fugacities are proportional to the amplitude for making a transition between two different atomic states. When the amplitude for making transitions between states of different charge grows as we go towards longer time scales the system is a Fermi liquid. When this amplitude renormalizes to zero, quantum coherence is destroyed and Fermi-liquid-theory breaks down. We cast the breakdown of Fermi-liquid theory in the framework of the macroscopic quantum tunneling (MQT) problem.[14] The transitions between Fermi-liquid and non-Fermi-liquid phases are extensions of the well-known localization transitions in the MQT problem with one essential difference (responsible for a richer phase diagram): we deal with a special *three-level* system describing the local spin and charge degrees of freedom instead of the canonical *two-level* system studied in the MQT literature.

The possible phases are determined from the possible fixed points of the RG. We carry out the analysis of a more general SU(N) impurity model. The case $N=2$ corresponds to the three-level system [empty site and SU(2) spin]. We identify, besides the strong-coupling phase in which all excitations are coherent and the weak-coupling phase in which all excitations are incoherent, a new class of metallic state of matter in which spin excitations are coherent, while charge excitations are incoherent. We call this an intermediate-coupling phase. Both the intermediate-coupling and weak-coupling phases correspond to incoherent metallic states with vanishing quasiparticle residue, self-similar local correlation functions, and asymptotically decoupled charge and spin excitations. The low-energy behaviors are not described by Fermi-liquid theory.

The $N=1$ case reduces to the well-studied resonant level model.[15,16] It is well known that orthogonality effects are more pronounced when there are bound states, which can violate the unitarity bounds of the coupling

constants, or in the presence of many channels of conduction electrons.[17] This later point is emphasized by Ruckenstein and Varma in the search of a mechanism for marginal Fermi-liquid states in realistic models. Along this line, Giamarchi *et al.* have recently suggested that an impurity model containing a bath with *several channels* of screening electrons is closely related to the copper oxides.[18] More recently Perakis *et al.* suggested that the presence of several channels of screening electrons can give rise to non-Fermi-liquid behavior similar to the one found in the multichannel Kondo problem.[19] The addition of extra channels of conduction electrons[20] in our formalism amounts to a change in the initial conditions of the renormalization-group flow.

The paper is organized as follows. In Sec. II A, we introduce the extended Hubbard model and derive, in the limit of infinite dimensions, the associated impurity problem in a self-consistent medium. This impurity problem is a generalized asymmetric Anderson model. The qualitative physics associated with such an impurity problem is discussed in Sec. II B. The justification for the associated impurity problem being near criticality is given in Sec. II C. In Sec. III A, we construct the atomic expansion for the partition function of the impurity problem. The resultant partition function is a summation over histories of the local degrees of freedom. It is shown in Sec. III B that, this partition function corresponds to a particular realization of a class of one-dimensional classical spin models with long-range interactions considered by Cardy,[21] extended to account for a symmetry breaking field. Using Cardy's procedure, we derive in Sec. IV the renormalization-group equations, and analyze the resulting universality classes and crossover behavior. In Sec. V we establish the nature of the Fermi-liquid and the non-Fermi-liquid phases of the extended Hubbard model. A summary of the phase diagram is given in Sec. V C. In Sec. V D, we establish the relevance of our results to models with more realistic densities of states. In Sec. VI we conclude with a discussion of the relevance of our results to realistic finite-dimensional systems. The paper includes three appendixes. Appendix A summarizes the bosonization procedure. Appendix B gives the details of the derivation of the renormalization-group equations. Finally, in Appendix C, we derive the correlation functions in the weak-coupling mixed-valence regime. A brief account of the renormalization-group flow and its implication for the extended Hubbard model in infinite dimensions has been given in Ref. 22.

II. THE EXTENDED HUBBARD MODEL IN INFINITE DIMENSIONS

A. The extended Hubbard model in infinite dimensions and its associated impurity model

We study the following extended Hubbard model

$$H = \sum_{ij} \sum_{\sigma=1}^{N} (t_{ij} - \mu\delta_{ij})c_{i\sigma}^{\dagger}c_{j\sigma} + \sum_{i} \sum_{\sigma=1}^{N} (\epsilon_d^0 - \mu)d_{i\sigma}^{\dagger}d_{i\sigma} + \frac{U}{2} \sum_{i} \sum_{\sigma\neq\sigma'} d_{i\sigma}^{\dagger}d_{i\sigma}d_{i\sigma'}^{\dagger}d_{i\sigma'}$$
$$+ \sum_{i} \sum_{\sigma=1}^{N} t(d_{i\sigma}^{\dagger}c_{i\sigma} + \text{H.c.}) + \frac{V_1}{N} \sum_{i} \sum_{\sigma,\sigma'} c_{i\sigma}^{\dagger}c_{i\sigma}d_{i\sigma'}^{\dagger}d_{i\sigma'} + \frac{V_2}{N} \sum_{i} \sum_{\sigma,\sigma'} c_{i\sigma}^{\dagger}c_{i\sigma'}d_{i\sigma'}^{\dagger}d_{i\sigma} . \tag{1}$$

It includes two species of electrons. The uncorrelated conduction c electrons have the hopping matrix t_{ij} or, equivalently, the dispersion ϵ_k. The localized d electrons have an energy level ϵ_d^0 and on-site Coulomb interaction U, which is taken to be infinity. These two species of electrons are coupled, at every site, through a hybridization t, a density-density interaction V_1/N, and a spin exchange interaction V_2/N. For generality, we work with arbitrary spin degeneracy N, which will also allow us to make contact with results from large N expansion. Finally, the chemical potential is μ.

In the spinless case $(N=1)$ this model is reduced to a generalized Falicov-Kimball model, which includes, besides the usual interaction V_1, a hybridization t term. In the limit of vanishing hybridization, the Falicov-Kimball model is exactly soluble in infinite dimensions.[23,24] When the density of states is a Lorentzian[25,8] all the correlation functions can be computed analytically and the origin of the breakdown of Fermi-liquid theory in the model can be understood in simple physical terms.[26] There is a range of electron densities where the chemical potential coincides with the position of the renormalized d electron level. We referred to that situation as the pinning of the

chemical potential. We notice, however, that the Falicov-Kimball model should be understood as the zero hybridization limit of the model (1).[26] In this paper we show that there are regions of parameter space in which the hybridization dynamically renormalizes to zero at low energies and establish that the Falicov-Kimball fixed point in the pinned region has a finite basin of attraction.

The spin-$\frac{1}{2}$ case $(N=2)$ is a version of the extended Hubbard model first studied in the context of the mixed valence problem.[27] It has some similarities with the extended Hubbard model relevant to the high-T_c systems proposed by Emery[28] and Varma, Schmitt-Rink, and Abrahams.[29]

The infinite dimension limit of a lattice fermion model is defined through an appropriate scaling of the hopping term,[7] which in our case is that of the conduction electrons. It has been shown that one can naturally associate with each lattice model in infinite dimensions an impurity model. This impurity model is obtained by integrating out all the degrees of freedom except for those living at the origin.[8,9]

Following this procedure we obtain the single-site effective action of our extended Hubbard model:

$$S_{\text{site}}(G_0) = -\int_0^\beta d\tau \int_0^\beta d\tau' \psi^\dagger(\tau) G_0^{-1}(\tau-\tau')\psi(\tau')$$
$$+ \int_0^\beta d\tau \left[\frac{V_1}{N} \sum_{\sigma,\sigma'} c_\sigma^\dagger c_\sigma d_{\sigma'}^\dagger d_{\sigma'} + \frac{V_2}{N} \sum_{\sigma,\sigma'} c_\sigma^\dagger c_{\sigma'} d_{\sigma'}^\dagger d_\sigma + \frac{U}{2} \sum_{\sigma\neq\sigma'} d_\sigma^\dagger d_\sigma d_{\sigma'}^\dagger d_{\sigma'} \right] , \tag{2}$$

where $\psi^\dagger = (c^\dagger, d^\dagger)$. The Weiss effective field G_0^{-1} is a 2×2 matrix. It describes the effect of all the Feynman trajectories in which the electron at site zero leaves the origin, explores the lattice, and returns to the origin. Translational invariance demands that all the local correlation functions of the lattice model are the same as the correlation functions of the impurity model leading to the following self-consistency equations:

$$\int_{-\infty}^\infty d\epsilon N_0(\epsilon) \begin{bmatrix} i\omega_n + \mu - \epsilon - \Sigma_{cc}^{\text{imp}} & t - \Sigma_{cd}^{\text{imp}} \\ t - \Sigma_{dc}^{\text{imp}} & i\omega_n + \mu - \epsilon_d^0 - \Sigma_{dd}^{\text{imp}} \end{bmatrix}^{-1} = \begin{bmatrix} (G_0^{-1})_{cc} - \Sigma_{cc}^{\text{imp}} & (G_0^{-1})_{cd} - \Sigma_{cd}^{\text{imp}} \\ (G_0^{-1})_{dc} - \Sigma_{dc}^{\text{imp}} & (G_0^{-1})_{dd} - \Sigma_{dd}^{\text{imp}} \end{bmatrix}^{-1} . \tag{3}$$

Here the noninteracting density of states, $N_0(\epsilon) = (N_{\text{site}})^{-1}\Sigma_k \delta(\epsilon - \epsilon_k)$, where ϵ_k the conduction-electron dispersion, is the only place where the nature of the lattice enters. Σ^{imp} is a functional of G_0 defined by the self-energy matrix of the single-site impurity model defined in Eq. (2). After solving the system of equations (2) and (3) for G_0 we can evaluate the self-energy of the lattice model $\Sigma = \Sigma_{\text{imp}}(G_0)$.

For a Lorentzian density of states, G_0 can be solved explicitly:[8,26]

$$\begin{bmatrix} (G_0^{-1})_{cc} & (G_0^{-1})_{cd} \\ (G_0^{-1})_{dc} & (G_0^{-1})_{dd} \end{bmatrix} = \begin{bmatrix} i\omega_n + \mu + i\Gamma\,\text{sgn}\omega_n & t \\ t & i\omega_n + \mu - \epsilon_d^0 \end{bmatrix} , \tag{4}$$

where Γ is the width of the Lorentzian. A more general density of states, however, does not alter the qualitative results derived here, provided that the system is metallic and the hybridization t is smaller than the bandwidth of the conduction electrons. This will be discussed further in Sec. V D.

Our single-site action describes an impurity model:

$$S_{\text{imp}} = \int_0^\beta d\tau \sum_{k\sigma} c_{k\sigma}^\dagger (\partial_\tau + \mu - \epsilon_k)c_{k\sigma} + d_\sigma^\dagger (\partial_\tau + \mu - \epsilon_d^0)d_\sigma + \sum_\sigma t(d_\sigma^\dagger c_\sigma + \text{H.c.})$$
$$+ \frac{V_1}{N} \sum_{\sigma,\sigma'} c_\sigma^\dagger c_\sigma d_{\sigma'}^\dagger d_{\sigma'} + \frac{V_2}{N} \sum_{\sigma,\sigma'} c_\sigma^\dagger c_{\sigma'} d_\sigma^\dagger d_\sigma + \frac{U}{2} \sum_{\sigma\neq\sigma'} d_\sigma^\dagger d_\sigma d_{\sigma'}^\dagger d_{\sigma'} , \tag{5}$$

where an electron bath, with dispersion ϵ_k, has been introduced to generate the Weiss field G_0^{-1} given in Eq. (4). This is the generalized Anderson impurity model.

B. Qualitative physics of the generalized Anderson model

The Hamiltonian of the generalized Anderson impurity problem corresponding to the action in Eq. (5) is given by

$$H_{\mathrm{imp}} = \sum_{k\sigma} E_k c_{k\sigma}^{\dagger} c_{k\sigma} + E_d^0 d_{\sigma}^{\dagger} d_{\sigma} + \sum_{\sigma} t\, (d_{\sigma}^{\dagger} c_{\sigma} + \mathrm{H.c.})$$

$$+ \frac{V_1}{N} \sum_{\sigma,\sigma'} c_{\sigma}^{\dagger} c_{\sigma} d_{\sigma'}^{\dagger} d_{\sigma'} + \frac{V_2}{N} \sum_{\sigma,\sigma'} c_{\sigma}^{\dagger} c_{\sigma'} d_{\sigma'}^{\dagger} d_{\sigma} + \frac{U}{2} \sum_{\sigma \neq \sigma'} d_{\sigma}^{\dagger} d_{\sigma} d_{\sigma'}^{\dagger} d_{\sigma'} , \tag{6}$$

where the d electron level

$$E_d^0 = \epsilon_d^0 - \mu \tag{7}$$

and the bath electron dispersion $E_k = \epsilon_k - \mu$.

In this subsection, we give a qualitative discussion of the physics associated with this model. We separate the discussion for the spinless and spinful cases.

In the spinless case ($N = 1$) this model is reduced to the resonant level model. It was previously established[15,16] that the resonant level model can be mapped onto an anisotropic spin-$\frac{1}{2}$ Kondo problem through the following: (a) the hybridization t is identified with the transverse Kondo exchange $\frac{1}{2} J_{\perp}$; (b) the density-density interaction V_1, when written in a particle-hole symmetric form, is related to the longitudinal component of the Kondo exchange $J_{\parallel}$ through identifying the corresponding phase shifts: $(1 - 2\delta/\pi)^2 \rightarrow 2(1 - 2\delta_{\parallel}/\pi)^2$, where $\delta = \tan^{-1}(\pi\rho_0 V_1/2)$ and $\delta_{\parallel} = \tan^{-1}(\pi\rho_0 J_{\parallel}/4)$, with ρ_0 the conduction electron density of states at the Fermi level; and (c) the d electron level E_d^0 is mapped onto the magnetic field $(-H)$ applied on the local moment. Such a mapping allows a parallel discussion of the qualitative physics of the resonant level model and that of the Kondo problem.

We recall that, at zero magnetic field, the Kondo problem has weak-coupling fixed points when the exchange coupling is ferromagnetic: the transverse Kondo exchange is renormalized to zero. For an antiferromagnetic exchange coupling, it flows to a strong coupling fixed point.[30,31] The transition can be viewed as an unbinding of defects (*spin flips*) in the path integral representation for the partition function to be described in Sec. III, as in the Kosterlitz-Thouless transition of the two-dimensional (2D) XY model.[32,33] In complete analogy, when the d level is located at the chemical potential, the resonant level model has a weak-coupling fixed line for a range of attractive interactions given by $2\delta/\pi < -(\sqrt{2} - 1)$.[15,16] The hybridization becomes relevant for $2\delta/\pi > -(\sqrt{2} - 1)$, at which a strong-coupling phase emerges at low energies. The zero-temperature transition between these phases involves the unbinding of defects describing transitions between states with different charge (*charge flips*) in the path integral representation of the partition function to be described in Sec. III.

Applying a large magnetic field at the impurity in the Kondo problem polarizes the impurity spin, cuts off the infrared singularities, and therefore destroys the Kondo process. Similarly in the resonant level model, when the d level is far away from the chemical potential, the d orbital is either fully occupied or empty, and the resonant level model becomes a potential scattering problem. Interesting physics occurs in the mixed valence regime, when the renormalized d level, denoted as E_d^*, is close to zero.

The nature of these fixed points can also be discussed in parallel. In the ferromagnetic Kondo problem in zero magnetic field, the spectrum is composed of conduction electrons and a local spin mode, which are asymptotically decoupled at low energies. There is no energy scale in the problem; correlation functions have long-time algebraic behavior and do not have the Fermi-liquid form. Similarly the spectrum of the resonant level model in the weak-coupling regime, when the d level is located at the Fermi energy of the conduction electrons, is composed of the local d electron and the conduction electrons, which are asymptotically decoupled. The d electron spectral function, as well as local correlation functions, exhibit power-law behavior in frequency with interaction-dependent exponents, due to the finite value of the renormalized density-density interaction V_1^*. The divergence occurs at zero frequency when $E_d^* = 0$. In both cases, the low-energy excitations are incoherent and cannot be analytically continued to those of noninteracting electron systems.

In the antiferromagnetic Kondo problem, the local spin mode is quenched below the Kondo energy scale T_K through the formation of quasiparticles, which correspond to coherent spin excitations. In the resonant level model at the strong-coupling regime, the renormalized hybridization t^* between the local d and conduction electrons is finite. This renormalized hybridization sets the energy scale, below which the local d electron *retains* its free-electron character and combines with the conduction electrons to form quasiparticles. These quasiparticles describe coherent charge excitations. In both cases, the low-energy behavior is described by a Fermi liquid.

The above discussion indicates that, whether or not the hybridization is relevant determines the nature of the low-energy behavior. This point can be further seen by noticing that the wave-function renormalization factor associated with the d electron is equivalent to the renormalization of the hybridization: therefore, whether or not the renormalized hybridization is nonzero determines the existence or vanishing of the quasiparticle residue. This motivates us to study the flow of the hybridization, along with other couplings.

For a spinful case ($N \geq 2$) the generalized Anderson model has low-energy excitations in both the charge and spin channel. We will show, using the RG flow, that the interplay between charge and spin dynamics leads to three kinds of mixed valence states, characterized by

different ways the hybridization and the exchange coupling are renormalized.

Strong coupling mixed valence fixed point. Both the hybridization and exchange coupling are relevant. As in the antiferromagnetic Kondo problem and in the strong-coupling regime of the resonant level model, the spectral functions at low energies are described in terms of a resonance around the chemical potential. The width of the resonance sets the scale for the low-energy coherent quasiparticle excitations. This is in the same universality class as the usual strong-coupling phase of the Anderson model.

Weak coupling mixed valence fixed points. Both the hybridization and the exchange couplings are irrelevant. The system is self-similar; correlation functions in the charge and spin channels have algebraic behavior similar to those of the ferromagnetic Kondo problem and of the weak-coupling regime of the resonant level model, respectively. Both the charge and spin excitations are incoherent.

Intermediate coupling mixed valence fixed points. Here, the hybridization is irrelevant, while the exchange coupling is relevant. The system is self-similar in the charge channel, and exhibits a finite-energy scale in the spin channel. The correlation functions in the charge channel have an algebraic behavior similar to those of the weak-coupling regime of the resonant level model, while the correlation functions in the spin channel are characterized by a resonance in analogy to those of the antiferromagnetic Kondo problem. Therefore, the low-energy charge excitations are incoherent, the low-energy spin excitations are coherent.

The intermediate mixed valence phase occurs because the two kinds of defects (spin flips and charge flips) can unbind at different stages.[35] We will establish that, due to the special form of the coupling between the spin and charge dynamics, a phase with coherent charge excitations and incoherent spin excitations cannot exist.

C. Pinning of the local states at chemical potential

In this subsection we show that the fact that the impurity model is the result of a mapping from a lattice model forces the impurity to be near criticality over a range of parameters.

The local Green's functions of a lattice fermion model in infinite dimensions are given by those of the impurity problem. Therefore, the density of d electrons plus the local density of c electrons in the ground state of the impurity model Eq. (6) equals the total electron density (n) of the original lattice problem Eq. (1):

$$\sum_\sigma \langle d_\sigma^\dagger d_\sigma \rangle + \sum_\sigma \langle c_{0,\sigma}^\dagger c_{0,\sigma} \rangle = n . \tag{8}$$

To determine n_d within the impurity model Eq. (6), we first note that the d level is renormalized from its bare value. This happens due to two sources, a short-time Hartree-like renormalization due to the interactions and a long-time contribution due to the hybridization, which is described by the RG flow of Sec. V.

To study the short-time renormalization, we consider the nonflipping part of the Hamiltonian given in Appendix A. The shift of the d level ΔE_d comes from the change of the ground-state energy of the conduction electron sea, when a d electron is present. The renormalized d level is given by

$$\widetilde{E}_d(\mu) = \epsilon_d^0 - \mu + \Delta E_d(\mu) . \tag{9}$$

Here ΔE_d depends on the chemical potential μ since the shift of the ground-state energy changes as μ is varied.

There exists a critical chemical potential, $\mu = \mu_c^0$, at which the renormalized d level lies at the chemical potential,

$$\widetilde{E}_d(\mu_c^0) = 0 . \tag{10}$$

In the absence of hybridization, such a condition indicates that, at $\mu = \mu_c^0$, the heavy electron lies right at the Fermi level of the electron bath. Both n_d and n_c jump as μ varies through μ_c. Therefore, *a finite range of electron densities* correspond to the chemical potential μ_c^0.[26] Over this range of the electron densities, the d level is pinned at the chemical potential. Within this pinned density range, there is no energy barrier for the transition from one local charge state to another.

The essential question is whether, when the hybridization term is present, the chemical potential can still be adjusted to a value μ_c so that the renormalized d level is equal to zero. In the language of critical phenomena, our procedure here is equivalent to renormalizing a massless field theory. In Sec. V, we will show through the RG analysis that this can indeed be achieved when the hybridization is irrelevant.

III. PARTITION FUNCTION OF THE GENERALIZED ANDERSON MODEL

We now turn to the RG analysis of the generalized Anderson model Eq. (6) near the mixed valence regime, where the renormalized d level is near the chemical potential.

To derive the RG flow, our strategy is to first construct an expansion around the atomic limit, in terms of the hopping amplitudes between the local atomic configurations. It leads to a partition function written as a summation over histories associated with the local degrees of freedom. This in turn is equivalent to a $(0+1)$-dimensional statistical mechanical model with long-range interactions between the flipping events. Such an atomic expansion originates in the work of Anderson and Yuval in the Kondo problem[30] and of Haldane in the asymmetric Anderson model.[13] Here we generalize it to arbitrary local configurations, and construct a closed set of RG equations. We stress that this atomic expansion is perturbative in the hoppings, but nonperturbative in the interactions and the symmetry-breaking fields.

To illustrate the methodology, we recall that RG equations for Kondo-like impurity problems have been derived using (a) poor man's scaling;[30,13] (b) multiplicative RG;[36] and (c) mapping to a one-dimensional statistical mechanical problem.[30,13] In the most general form, both the poor man's scaling and the multiplicative RG are

difficult to carry out systematically; many couplings are present, and it is not *a priori* clear which combinations of these couplings come into the flow. We will show that, for a general set of local configurations, the partition functions derived from the atomic expansion can be mapped onto a class of discrete classical spin-chain models with a long-range $1/r^2$ interaction in symmetry-breaking fields. This will allow us to carry out a systematic RG analysis in the general case, by generalizing Cardy's analysis of these models[21] to incorporate the symmetry-breaking fields. We note that Haldane's work[13] for the asymmetric Anderson model emphasizes the importance of a symmetry-breaking field (i.e., the impurity level) as a consequence of the lack of particle-hole symmetry. Since the focus is on identifying various regimes *within* the strong-coupling Fermi-liquid phase, scaling equations are constructed for the hybridization and the symmetry-breaking field only. In Cardy's work[21] for the general class of one-dimensional classical discrete spin chains with long-range interactions, RG flow is constructed for all coupling constants, but without incorporating the symmetry-breaking fields. The effect of the symmetry-breaking fields in this scheme has been studied previously in other context.[37] For our purposes of identifying different low-energy fixed points and the associated transitions and/or crossovers between them, it is essential to study the renormalization of all the coupling constants in the generalized Anderson model. Meanwhile, particle-hole asymmetry generates nonzero effective fields even if we start from zero values of the bare fields. By combining the formalism used in the works of Haldane and Cardy, we are able to derive the systematic RG equations for the generalized Anderson model near criticality, and identify and study Fermi-liquid and non-Fermi-liquid phases.

In this section, we give the details of the atomic expansion for the partition function of the generalized Anderson model. In the next section, we derive the RG flow and establish the nature of the resulting fixed points.

A. The partition function as a summation over histories

For the generalized Anderson model at $U = \infty$,[38] the local degrees of freedom are characterized by the $N+1$ d-electron states, $|\alpha\rangle = |0\rangle$, or $|\sigma_m\rangle$ for $m = 1, \ldots, N$. To perform the atomic expansion, we first separate the impurity Hamiltonian into two parts

$$H = H_0 + H_f , \tag{11}$$

where H_0 is diagonal in the space of the local states:

$$H_0 = \sum_{k\sigma} E_k c_{k\sigma}^\dagger c_{k\sigma} + E_d^0 d_\sigma^\dagger d_\sigma + \frac{U}{2} \sum_{\sigma \neq \sigma'} d_\sigma^\dagger d_\sigma d_{\sigma'}^\dagger d_{\sigma'}$$
$$+ \frac{V_1}{N} \sum_{\sigma,\sigma'} c_\sigma^\dagger c_\sigma d_{\sigma'}^\dagger d_{\sigma'} + \frac{V_2^\parallel}{N} \sum_\sigma c_\sigma^\dagger c_\sigma d_\sigma^\dagger d_\sigma . \tag{12}$$

The remaining part

$$H_f = \sum_\sigma t(d_\sigma^\dagger c_\sigma + \text{H.c.}) + \frac{V_2^\perp}{N} \sum_{\sigma,\sigma' \neq \sigma} d_\sigma^\dagger d_{\sigma'} c_{\sigma'}^\dagger c_\sigma \tag{13}$$

flips from one local state to another.

We can write H_0 in terms of the projection operators $X_{\alpha\alpha} = |\alpha\rangle\langle\alpha|$,

$$H_0 = \sum_\alpha H_\alpha X_{\alpha\alpha} , \tag{14}$$

where

$$H_\alpha = E_\alpha + \sum_\gamma V_\alpha^\gamma c_\gamma^\dagger c_\gamma + \sum_{k\gamma} E_k c_{k\gamma}^\dagger c_{k\gamma} . \tag{15}$$

Here $c_\gamma^\dagger$ creates a Wanniar state of the conduction electrons of spin γ at the impurity site. The local levels are $E_0 = 0$, $E_\sigma = E_d^0$, and the potentials are given by

$$V_\sigma^\gamma = \frac{V_1}{N} + \frac{V_2^\parallel}{N} \delta_{\gamma\sigma} , \tag{16}$$
$$V_0^\gamma = 0 .$$

Meanwhile, the flipping part can be decomposed as follows:

$$H_f = \sum_{\alpha \neq \beta} Q(\alpha,\beta) , \tag{17}$$

where

$$Q(\alpha,\beta) = |\alpha\rangle\langle\alpha|H_f|\beta\rangle\langle\beta| \tag{18}$$

describes the process flipping from the local state $|\beta\rangle$ into $|\alpha\rangle$. Specifically,

$$Q(\sigma,0) = Q^\dagger(0,\sigma) = t d_\sigma^\dagger c_\sigma ,$$
$$Q(\sigma,\sigma') = \frac{V_2^\perp}{N} d_\sigma^\dagger d_{\sigma'} c_{\sigma'}^\dagger c_\sigma (1 - \delta_{\sigma\sigma'}) . \tag{19}$$

The partition function

$$Z = \int DcDd \exp\left[- \left[S_0 + \int_0^\beta d\tau H_f(\tau) \right] \right] \tag{20}$$

can be expanded in H_f

$$Z = \sum_{n=0}^\infty \int_0^\beta d\tau_n \cdots \int_0^{\tau_{i+1}} d\tau_i \cdots \int_0^{\tau_2} d\tau_1 \sum_\alpha A(\alpha; \tau_n, \ldots, \tau_1) , \tag{21}$$

where the transition amplitude, for a given initial (and final) state $|\alpha\rangle$ and a sequence of flipping times $\tau_1 < \cdots < \tau_n$, is given by

$$A(\alpha; \tau_n, \ldots, \tau_1) = (-1)^n \int DcDd \langle\alpha|T[\exp(-\beta H_0)H_f(\tau_n) \cdots H_f(\tau_i) \cdots H_f(\tau_1)]|\alpha\rangle . \tag{22}$$

For each transition amplitude, the path integral over the d states can be carried out through inserting a complete set of local states at every discrete imaginary time, leading to

$$A(\alpha;\tau_n, \ldots, \tau_1) = (-1)^n \sum_{\alpha_2, \ldots, \alpha_n} \int Dc \exp[-H_\alpha(\beta - \tau_n)] Q'(\alpha, \alpha_n) \cdots$$

$$\times \exp[-H_{\alpha_{i+1}}(\tau_{i+1} - \tau_i)] Q'(\alpha_{i+1}, \alpha_i) \exp[-H_{\alpha_i}(\tau_i - \tau_{i-1})] \cdots$$

$$\times \exp[-H_{\alpha_2}(\tau - \tau_1)] Q'(\alpha_2, \alpha) \exp[-H_\alpha \tau_1] . \tag{23}$$

Here, $\alpha, \alpha_2, \ldots, \alpha_n$ and $\tau_1, \ldots, \tau_n$ label a Feynman trajectory: the local configuration starts from $|\alpha_1\rangle = |\alpha\rangle$, changes from $|\alpha_i\rangle$ to $|\alpha_{i+1}\rangle$ at time τ_i, $(i=1, \ldots, n-1)$, and returns to $|\alpha_{n+1}\rangle = |\alpha\rangle$ at τ_n. This is illustrated in Fig. 1.

The flipping operator $Q'(\alpha_{i+1}, \alpha_i) = \langle \alpha_{i+1}|H_f|\alpha_i\rangle$ can be separated as follows:

$$\langle \alpha|H_f|\beta\rangle = y'_{\alpha\beta} O'(\alpha, \beta) . \tag{24}$$

Here $y'_{\alpha\beta}$ is the hopping amplitude associated with the flipping event (α, β): $y'_{0,\sigma} = y'_{\sigma,0} = t$, $y'_{\sigma,\sigma'} = V_{\frac{1}{2}}^{\perp}/N$. $O'(\alpha, \beta)$ is composed of conduction-electron operators, which describe the distortion in the sea of conduction electrons associated with the flipping event: $O'(\sigma, 0) = O'^{\dagger}(0, \sigma) = c_\sigma$ and $O'(\sigma, \sigma') = c_{\sigma'}^{\dagger} c_\sigma$. It is the reaction of the conduction-electron bath to these local distortions, which will renormalize the hopping amplitude as we go to lower energies.

We can now trace out the conduction-electron degrees of freedom. The complication in evaluating each transition amplitude lies in the fact that it has a history-dependent potential. This can be dealt with most conveniently through the bosonization procedure.[39,3] The relevant details of the bosonization applied to the impurity problems is summarized in Appendix A. We retain only the S-wave component of the conduction electrons, which can be represented by

$$c_\sigma(x) = \frac{1}{\sqrt{2\pi a}} e^{-i\Phi_\sigma(x)} , \tag{25}$$

where the Φ_σ field is defined in Appendix A. The radial dimension x has been extended to the negative half axis. Hence, only one chiral component of the Tomonaga boson is introduced.

The projected Hamiltonian transforms into

$$H_\alpha = H_c + E'_\alpha + \sum_\gamma \frac{\delta_\alpha^\gamma}{\pi\rho_0} \left[\frac{d\Phi_\gamma}{dx} \right]_{x=0} , \tag{26}$$

where ρ_0 is the bare conduction electron density of states at the Fermi level. The phase shifts δ_α^γ are determined by the scattering potentials defined in Eq. (16),

$$\delta_\sigma^\gamma = \delta_1 + \delta_2 \delta_{\gamma\sigma} , \tag{27}$$

$$\delta_0^\gamma = 0 ,$$

where

$$\delta_1 = \tan^{-1}(\pi\rho_0 V_1/N) ,$$

$$\delta_2 = \tan^{-1}(\pi\rho_0 V_{\frac{1}{2}}^{\parallel}/N) . \tag{28}$$

All the short-time dynamics (for τ smaller than ξ_0) are included in the shift of the atomic level, leading to the renormalized levels $E'_\alpha = E_\alpha + \Delta E_\alpha$. The details for this level shift are given in Appendix A.

The history-dependent potential is treated through introducing a canonical transformation[39] at each imaginary time

$$U_\delta = \exp(i\delta\Phi) . \tag{29}$$

The transformed potential is time independent, due to the following property:

$$U_\delta^{\dagger} H_c U_\delta = H_c + \frac{\delta}{\pi\rho_0} \left[\frac{d\Phi}{dx} \right]_{x=0} . \tag{30}$$

It is important to note that, the unitary transformation operator given in Eq. (29) has the same form as the fermion operators. The transition amplitude now reduces to[40]

$$A(\alpha;\tau_n, \ldots, \tau_1) = Z_c \sum_{\alpha_{n+1} = \alpha_1 = \alpha, \alpha_2, \ldots, \alpha_n} y'_{\alpha_{n+1}, \alpha_n} \cdots y'_{\alpha_{i+1}, \alpha_i} \cdots y'_{\alpha_2, \alpha_1}$$

$$\times \exp\left[-E'_\alpha(\tau_1 - \tau_n) - \sum_{i=2}^{n-1} E'_{\alpha_{i+1}}(\tau_{i+1} - \tau_i) \right]$$

$$\times \langle O(\alpha_{n+1}, \alpha_n)(\tau_n) \cdots O(\alpha_{i+1}, \alpha_i)(\tau_i) \cdots O(\alpha_2, \alpha_1)(\tau_1) \rangle . \tag{31}$$

Here

$$O(\alpha_{i+1}, \alpha_i)(\tau_i) \equiv \exp(H_c \tau_i) O(\alpha_{i+1}, \alpha_i) \exp(-H_c \tau_i) , \tag{32}$$

where the disorder operators are given by

$$O(\alpha_{i+1}, \alpha_i) = (\Pi_\gamma U_{\delta_{\alpha_{i+1}}^\gamma}) O'(\alpha_{i+1}, \alpha_i) (\Pi_\gamma U_{\delta_{\alpha_i}^\gamma}^{\dagger}) . \tag{33}$$

It is the product of the canonical transformation operators, which represent the physics of a time-dependent potential,

and the conduction electron operators reflecting the distortion in the conduction electron sea. In terms of the boson fields,

$$O(0,\sigma)=\exp[i(1-\delta_2/\pi)\Phi_\sigma]\exp\left[-i\sum_\gamma(\delta_1/\pi)\Phi_\gamma\right],$$

$$O(\sigma,\sigma')=\exp[i(1-\delta_2/\pi)\Phi_{\sigma'}]\exp[-i(1-\delta_2/\pi)\Phi_\sigma].\tag{34}$$

Equations (34) specify the initial values for the anomalous dimension $e_{\alpha\beta}^\gamma$ of the disorder operator

$$O(\alpha,\beta)\equiv\exp\left[i\sum_\gamma e_{\alpha\beta}^\gamma\Phi_\gamma\right].\tag{35}$$

Specifically,

$$e_{0,\sigma}^\gamma=-e_{0,\sigma}^\gamma=\left[1-\frac{\delta_2}{\pi}\right]\delta_{\gamma,\sigma}-\frac{\delta_1}{\pi},$$

$$e_{\sigma,\sigma'}^\gamma=-\left[1-\frac{\delta_2}{\pi}\right]\delta_{\gamma,\sigma}+\left[1-\frac{\delta_2}{\pi}\right]\delta_{\gamma,\sigma'}.\tag{36}$$

Combining Eqs. (21) and (31), we arrive at

$$\frac{Z}{Z_0}=\sum_{n=0}^\infty\sum_{\alpha_{n+1}=\alpha_1,\ldots,\alpha_n}\int_{\xi_0}^{\beta-\xi_0}\frac{d\tau_n}{\xi_0}\cdots\int_{\xi_0}^{\tau_{i+1}-\xi_0}\frac{d\tau_i}{\xi_0}\cdots\int_{\xi_0}^{\tau_2-\xi_0}\frac{d\tau_1}{\xi_0}A(\tau_n,\ldots,\tau_1)y_{\alpha_{n+1},\alpha_n}\cdots y_{\alpha_{i+1},\alpha_i}\cdots y_{\alpha_2,\alpha_1}$$

$$\times\exp\left[-\sum_i h_{\alpha_{i+1}}^0\frac{(\tau_{i+1}-\tau_i)}{\xi_0}\right],\tag{37}$$

where the transition amplitude

$$A(\tau_n,\ldots,\tau_1)=\langle O(\alpha_{n+1},\alpha_n)(\tau_n)\cdots O(\alpha_{i+1},\alpha_i)(\tau_i)\cdots O(\alpha_2,\alpha_1)(\tau_1)\rangle$$

$$=\frac{1}{Z_c}\int\exp\left[-S_c+\int_0^\beta D\tau'\sum_m j_m(\tau')\Phi_\gamma(\tau')\right]$$

$$=\exp\left[-\int D\tau'D\tau''\sum_\gamma j_\gamma(\tau')j_\gamma(\tau'')\langle\Phi_\gamma(\tau')\Phi_\gamma(\tau'')\rangle\right]\tag{38}$$

with the "source current"

$$j_\gamma(\tau)=\sum_{i=1}^n\delta(\tau-\tau_i)e_{\alpha_{i+1},\alpha_i}^\gamma.\tag{39}$$

In Eq. (37), the cutoff is explicitly written in the integration range. Also the dimensionless form of the flipping amplitude has been introduced: $y_{\alpha_{i+1}\alpha_i}=y'_{\alpha_{i+1}\alpha_i}\xi_0$. Specifically, the charge and spin fugacities are given as follows:

$$y(0,\sigma)=y_t=t\xi_0,$$

$$y(\sigma\neq\sigma')=y_j=\frac{V^{\frac{1}{2}}}{N}\xi_0.\tag{40}$$

In deriving Eq. (37), we have also absorbed in Z_0, besides the free conduction-electron partition function Z_c, a shift in the ground-state energy such that $\Sigma_\alpha h_\alpha^0=0$. Specifically,

$$h_0^0=-E_d'\xi_0\frac{N}{(N+1)},$$

$$h_\sigma^0=E_d'\xi_0\frac{1}{(N+1)}.\tag{41}$$

Using the $\frac{1}{\tau}$ behavior[41] of the long-time correlation function for the Tomonaga bosons, we finally arrive at

$$\frac{Z}{Z_0}=\sum_{n=0}^\infty\sum_{\alpha_{n+1}=\alpha_1,\ldots,\alpha_n}\int_{\xi_0}^{\beta-\xi_0}\frac{d\tau_n}{\xi_0}\cdots\int_{\xi_0}^{\tau_{i+1}-\xi_0}\frac{d\tau_i}{\xi_0}\cdots\int_{\xi_0}^{\tau_2-\xi_0}\frac{d\tau_1}{\xi_0}\exp(-S[\tau_1,\ldots,\tau_n]),\tag{42}$$

where

$$S[\tau_1,\ldots,\tau_n]=\sum_{i<j}\sum_{\gamma}(e^{\gamma}_{\alpha_i\alpha_{i+1}})(e^{\gamma}_{\alpha_j\alpha_{j+1}})\ln\frac{(\tau_j-\tau_i)}{\xi_0}-\sum_i\ln(y_{\alpha_i\alpha_{i+1}})+\sum_i h_{\alpha_{i+1}}\frac{(\tau_{i+1}-\tau_i)}{\xi_0}\ .\tag{43}$$

The partition function is now a summation over all possible histories of the local degrees of freedom, which fluctuate between the $N+1$ local states $|\alpha\rangle$. Each history, labeled by $\{\alpha_1,\ldots,\alpha_n;\tau_1,\ldots,\tau_n\}$, is a sequence of transitions between the local states from α_1 through α_n taking place at the time $\tau_1<\cdots<\tau_n$, as illustrated in Fig. 1. The action Eq. (43) gives the statistical weight of such a history.

We can interpret Eq. (43) as that associated with the partition function of a plasma of kinks with logarithmic interactions. It has (multicomponent) charge $e^{\sigma}_{\alpha\beta}$ and fugacity $y_{\alpha\beta}$.

B. Equivalence to a discrete spin chain with long-range interactions

The partition function now has its action expressed as a summation over logarithmic interactions between the pairwise kinks. Each kink is a flip in the original "spin" space (i.e., the local states $|\alpha\rangle$). The logarithmic interactions between the kink pairs can therefore be transformed into interactions between the spins. It is straightforward to show that the action in Eq. (43) can be written in a symmetric form,

$$S[\tau_1,\ldots,\tau_n]=\sum_{i<j}[K(\alpha_i,\alpha_j)+K(\alpha_{i+1},\alpha_{j+1})-K(\alpha_i,\alpha_{j+1})-K(\alpha_{i+1},\alpha_j)]\ln\frac{(\tau_j-\tau_i)}{\xi_0}$$

$$-\sum_i\ln(y_{\alpha_i\alpha_{i+1}})+\sum_i h_{\alpha_{i+1}}\frac{(\tau_{i+1}-\tau_i)}{\xi_0}\ ,\tag{44}$$

which can then be transformed into a long-range interaction between the spins,

$$S[\tau_1,\ldots,\tau_n]=\sum_{i<j}K(\alpha_i,\alpha_j)\frac{\xi_0^2}{(\tau_j-\tau_i)^2}-\sum_i\ln(y_{\alpha_i\alpha_{i+1}})+\sum_i h_{\alpha_{i+1}}\frac{(\tau_{i+1}-\tau_i)}{\xi_0}\ ,\tag{45}$$

where the spins $|\alpha\rangle$ can be in $N+1$ components.

This transformed action is a special case of a class of discrete spin models with $1/r^2$ interactions considered by Cardy,[21] generalized to incorporate an effective field. The bare values of the stiffness constants $-K(\alpha,\beta)$ are determined by the bare values of the charges $e^{\sigma}_{\alpha\beta}$,

$$K(\alpha,\beta)=-\frac{1}{2}\sum_{\gamma}(e^{\gamma}_{\alpha,\beta})^2\ .\tag{46}$$

Specifically,

$$K(0,\sigma)\equiv-\epsilon_t\ ,$$
$$K(\sigma,\sigma')\equiv-\epsilon_j(1-\delta_{\sigma,\sigma'})\ ,\tag{47}$$

where the bare values of the charge and spin stiffness constants are

$$\epsilon_t^0=\frac{1}{2}\left[\left[1-\frac{\delta_2}{\pi}-\frac{\delta_1}{\pi}\right]^2+(N-1)\left[\frac{\delta_1}{\pi}\right]^2\right]\ ,$$
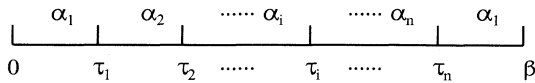$$\epsilon_j^0=\left[1-\frac{\delta_2}{\pi}\right]^2\ .\tag{48}$$

FIG. 1. Hopping sequences in the atomic representation. Here τ_i, for $i=1,\ldots,n$, labels the imaginary time at which the atomic configuration hops from $|\alpha_i\rangle$ to $|\alpha_{i+1}\rangle$.

IV. RG FLOW OF THE GENERALIZED ANDERSON MODEL AND THE NATURE OF THE FIXED POINTS

In this section, we derive the RG equations using the atomic representation of the partition function derived in the preceding section. The RG flow has the most general form in terms of the charge and spin fugacities, the charge and spin stiffness constants, and the d level (a symmetry breaking field). The flow equations enable us to identify all the fixed points. They correspond to a universal strong-coupling fixed point, a plane of weak-coupling fixed points, and a plane of intermediate-coupling fixed points. All these fixed points are studied in detail. We will establish in the next section that these fixed points describe Fermi-liquid and non-Fermi-liquid phases of the extended Hubbard model.

A. Renormalization-group equations

We construct RG equations for small E_d in this section. As was discussed in Sec. II C, in a certain range of parameters, the extended Hubbard model in infinite dimensions maps onto an impurity model, which has a zero renormalized mass (d level E_d). Therefore, the small E_d assumption is justified. However, since the RG procedure we use is perturbative in fugacities but nonperturbative in stiffness constants and fields, the RG equations for finite fields can also be constructed and are given in Appendix B.

The RG equations describe the flow of the dimensionless couplings as the bandwidth $1/\xi$ is reduced. The details of the derivations are presented in Appendix B,

where arbitrary local states with a partition function of the form given in Eqs. (42)–(45) are considered. For our $N+1$ local state problem, the RG charges are the charge and spin fugacities y_t and y_j [defined in Eq. (40)], the charge and spin stiffness constants ϵ_t and ϵ_j [defined in Eqs. (47) and (48)], and the dimensionless d level $E_d\xi = h_\sigma - h_0$. The RG equations are given as follows:

$$\frac{dy_t}{d\ln\xi} = (1-\epsilon_t)y_t + (N-1)y_t y_j \ ,$$

$$\frac{dy_j}{d\ln\xi} = (1-\epsilon_j)y_j + (N-2)y_j^2 + y_t^2 \ ,$$

$$\frac{d\epsilon_t}{d\ln\xi} = -2\epsilon_t(N+1)y_t^2 + \epsilon_j(N-1)(y_t^2 - y_j^2) \ ,$$

$$\frac{d\epsilon_j}{d\ln\xi} = -2\epsilon_j(y_t^2 + Ny_j^2) \ , \tag{49}$$

$$\frac{dE_d\xi}{d\ln\xi} = (N-1)(y_t^2 - y_j^2) + E_d\xi[1-(N+1)y_t^2] \ ,$$

$$\frac{dF\xi}{d\ln\xi} = F\xi - \frac{2N}{N+1}y_t^2 - \frac{N(N-1)}{N+1}y_j^2 \ ,$$

where F is the free energy.[42]

In the renormalization of the fugacitites, the linear terms give the associated anomalous dimensions, while the quadratic terms reflect the non-Abelian nature of our $N+1$ state problem. Physically, these cross terms reflect the coupling between the local spin and charge degrees of freedom. The renormalization of the stiffness constants reflects the correction to the interactions due to the fugacities of the charge and spin kinks.

In the renormalization of the energy level, the y_t^2 term arises because in integrating out the degrees of freedom the empty state gains a hybridization energy N times as much as a spin state does. This reflects the particle-hole asymmetry of the mixed-valence problem.[13] On the other hand, a spin state gains exchange energy through the other $(N-1)$ spin states, leading to the y_j^2 term. We emphasize that, the symmetry-breaking field is a relevant perturbation.

For $N=1$, the above RG equations reduce to those of the anisotropic Kondo problem, through identifying t with $\frac{1}{2}J_\perp$, ϵ_t with $[1-2/\pi\tan^{-1}(J_\parallel\xi_0/4)]^2$, and $-E_d$ with the magnetic field H applied on the local moment.[15,16] For $N=2$ and in the limit $V_1=V_2=0$, we reproduce equations of Haldane[13] for the flow of the d level and the hybridization for the asymmetric Anderson model in the mixed-valence regime.

B. Fixed points and critical behavior

The kinks are bound together when the amount of attraction between them are strong enough. This leads to fugacities renormalized to zero. As in the Kosterlitz-Thouless transition in the XY magnet,[32] unbinding of the kinks occurs when the attractions between the kinks become weak. In our case, ϵ_t and ϵ_j reflect the strength of the long-range interactions between the kinks. Since the spin and charge kinks are coupled, the unbinding of these kinks can occur either at the same time or at different

stages. The above RG equations lead to three kinds of fixed points. The phase diagram in the $\epsilon_t - \epsilon_j$ plane is given in Fig. 2.

The weak-coupling fixed points occur when both the spin and charge kinks are bound, corresponding to the hybridization and the exchange coupling both being irrelevant. This occurs when both the renormalized charge and spin stiffness constants are large enough,

$$\epsilon_t^* > 1 \ ,$$
$$\epsilon_j^* > 1 \ , \tag{50}$$

where the stiffness constants are renormalized from the bare values by the fugacities. To second order in the fugacities,

$$\epsilon_t^* = \epsilon_t^0 - (y_t^0)^2 \frac{2(N+1)\epsilon_t^0 - (N-1)\epsilon_j^0}{2(\epsilon_t^0-1)} - (y_j^0)^2 \frac{(N-1)\epsilon_j^0}{2(\epsilon_j^0-1)} \ , \tag{51}$$

$$\epsilon_j^* = \epsilon_j^0 - (y_t^0)^2 \frac{\epsilon_j^0}{\epsilon_t^0-1} - N(y_j^0)^2 \frac{\epsilon_j^0}{\epsilon_j^0-1} \ .$$

For $N=1$, this reduces to $\delta_1/\pi < -(\sqrt{2}-1)-t/\Gamma$.[15,16] For $N \geq 2$, it corresponds to

$$N\left[\frac{\delta_1}{\pi}\right]^2 - 2\left[1-\frac{\delta_2}{\pi}\right]\frac{\delta_1}{\pi} - \left[2-\left[1-\frac{\delta_2}{\pi}\right]^2\right] > 0 \ ,$$
$$\frac{\delta_2}{\pi} < 0 \ . \tag{52}$$

The strong-coupling mixed-valence fixed point occurs when both the spin and charge kinks are unbound, corresponding to the hybridization and the exchange coupling both being relevant. The basin of attraction is given by
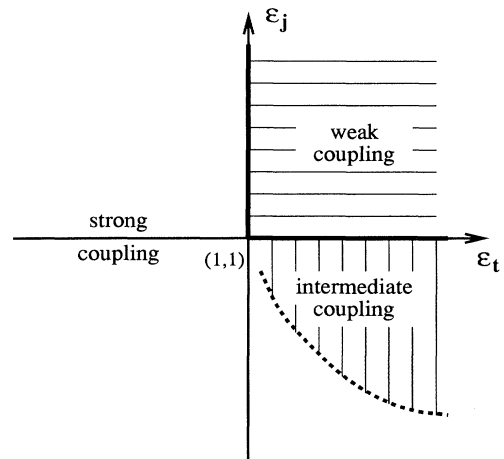
$$\epsilon_t^* < 1 \tag{53}$$

FIG. 2. Phase diagram of the generalized Anderson model in the mixed-valence regime. Here ϵ_t and ϵ_j label the charge and spin stiffness constants defined in the text. The vertical thick line, the horizontal thick line, and the dashed line are the boundaries between the strong-coupling, weak-coupling, and intermediate-coupling mixed-valence states.

and a range of $\epsilon_j^* < 1$ when $\epsilon_t^* > 1$.

This strong-coupling fixed point is beyond the reach of perturbative RG. It is, however, in the same universality class as the usual strong-coupling phase of the Anderson model: below a nonzero renormalized Fermi energy, both the local spin and charge degrees of freedom are quenched through the formation of quasiparticles.

In the spinful problem $(N \geq 2)$, for a range of couplings within the following domain,

$$\epsilon_t^* > 1 \,,$$

$$\epsilon_j^* < 1 \,,$$

(54)

an intermediate phase can occur for which the spin kinks are unbound, while the charge kinks are bound. Here the hybridization is irrelevant, while the exchange coupling is relevant. The local spins are quenched below a nonzero coherence energy, while the local charges are not. We note that the RG equations imply that when y_j becomes very large, it will start to drive y_t to increase. However, this late stage is beyond the reach of perturbative RG. We will establish in Sec. IV E that the fixed point with irrelevant y_t and relevant y_j is indeed stable. The transition to the strong-coupling phase occurs when the effective charge stiffness constants, further renormalized due to the unbound spin-kink plasma, reaches the critical value 1.

We emphasize that from the quadratic couplings in the scaling equations, a relevant charge coupling necessarily drives the spin coupling to be relevant, even with a bare $\epsilon_j > 1$. Physically, a spin kink (created by $d_\sigma^\dagger d_{\bar\sigma}$) is the composite of two charge kinks (created by d_σ). Unbounded charge kinks will strongly screen the interactions between the spin kinks, leading to the unbinding of the latter as well.

The phase boundaries are given in Fig. 2. The vertical thick line separates the weak-coupling phase from the strong-coupling phase. The horizontal thick line separates the weak-coupling phase from the intermediate-coupling phase. The (schematic) dashed line represents the boundary between the intermediate-coupling and strong-coupling phases.

We note the analogy of these three phases with those in the two-dimensional defect-driven melting problem.[35] There, the binding-unbinding transitions are associated with the dislocation and the disclination defects. A dislocation is the composite of a pair of disclinations, in analogy to the spin kink being a composite of a pair of charge kinks. The hexatic phase exhibits bound disclinations and unbound dislocations, in analogy to our intermediate coupling phase with irrelevant charge fugacity and relevant spin fugacity.

In terms of the physical interactions, i.e., the density-density interaction V_1 and the exchange interaction V_2, the basin of attraction of the weak-coupling fixed points corresponds to a range of attractive density-density and ferromagnetic exchange interactions, while the intermediate-coupling fixed points occur over a range of attractive density-density and antiferromagnetic Kondo exchange interactions. We stress that these are effective interactions at the beginning of the scaling trajectory. In

generic models in infinite dimensions with a non-Lorentzian density of state, there are high-energy dynamics, which have to be integrated out before the low-energy scaling regime is reached. We will discuss the implications of our results for more realistic models in Sec. VI.

We end this subsection with a discussion of the critical behavior of the zero-temperature quantum phase transitions between these various states we identified. For reasons to be described at the end, these zero-temperature quantum phase transitions can be formulated only in infinite dimensions. At finite dimensions we expect that the system will have sharp crossovers.

The transitions are characterized by the collapse of an energy scale,

$$\epsilon_F \sim \epsilon_0 e^{-1/(\epsilon - \epsilon_c)^\eta} \,.$$

(55)

The transition between the weak-coupling and strong-coupling mixed-valence states takes place when we vary the interactions (and, hence, ϵ_t^* and ϵ_j^*) through the vertical thick line in Fig. 2. This one-stage transition is illustrated in Fig. 3(a), where ϵ_1 labels a line in the $\epsilon_t - \epsilon_j$ plane that passes through the vertical thick line at ϵ_c. The RG equations imply that, the unbinding transition for spin kinks is driven by that of the charge kinks. The critical behavior is therefore determined by the renormalization of y_t only. Hence, ϵ_F in Eq. (55) corresponds to the Fermi energy of the Fermi liquid in the strong-coupling state, and the exponent $\eta = \frac{1}{2}$.

When we vary the interactions (and, hence, ϵ_t and ϵ_j) through the horizontal thick line and the dashed line in Fig. 2, two stages of transition take place, from the weak-coupling through the intermediate-coupling to the strong-coupling phase. This is illustrated in Fig. 3(b), where ϵ_2 labels a line in the $\epsilon_t - \epsilon_j$ plane that passes through the horizontal thick line at ϵ_{c2}, and through the dashed line at ϵ_{c1}. Near ϵ_{c2}, the ϵ_F in Eq. (55) refers to the coherence energy for coherent spin excitations in the
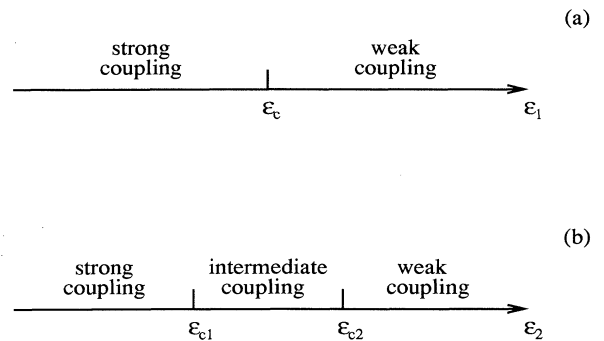
(a)

strong   weak
coupling   coupling
_____|_____→
        ϵ_c ϵ_1

(b)

strong   intermediate   weak
coupling   coupling   coupling
_____|_____|_____→
    ϵ_{c1} ϵ_{c2} ϵ_2

FIG. 3. Zero-temperature transition sequences when the interactions are varied such that within the ϵ_t-ϵ_j plane of Fig. 2, (a) a one-stage transition takes place from the weak-coupling to the strong-coupling state, and (b) two-stage transitions take place from the weak-coupling, through the intermediate-coupling, into the strong-coupling state. Here ϵ_c, ϵ_{c1}, and ϵ_{c2} label points on the vertical thick line, the horizontal thick line, and the dashed line, respectively, in Fig. 2.

intermediate coupling state. Close to ϵ_{c1}, on the other hand, ϵ_F refers to the coherence energy for the coherent charge excitations in the strong-coupling phase. The exponent characterizing the unbinding of spin kinks at ϵ_{c2} is given by $\eta = 1$. Due to rotational invariance, it differs from the exponent in the corresponding N-component Coulomb gas problem and is independent of N. The exponent characterizing the unbinding of charge kinks at ϵ_{c1}, on the other hand, is $\eta = \frac{1}{2}$.

In the following subsections, we discuss in detail the nature of these individual phases.

C. Strong-coupling mixed-valence state

Within the strong-coupling mixed valence state, both the hybridization and the exchange coupling are relevant. The effect of interactions becomes smaller as we go to lower energies. The nature of the fixed point is that of the strong-coupling mixed-valence state of the usual Anderson model. The ground state is well described by various variational wave functions, such as those of Varma and Yafet discussed in Ref. 27. The physics of this state can be systematically studied in the slave boson condensed phase in the large-N approach.[43] Within the strong coupling phase, there exist the empty-orbital, local-moment, and mixed-valence regimes.[13,34] Crossover between these various regimes occurs as the renormalized d level is varied with respect to the Fermi level.

In the following, we use our scaling equations to determine a generalized form for this d-level shift and resonance width $\Delta(\xi) = \pi y_t^2(\xi)/\xi$, in the presence of the finite density-density and exchange interactions. In the generic case, the flow of the d level can only be derived through integrating numerically the closed set of the RG flow. For a vanishing bare spin fugacity, $y_j^0 = 0$, and when the renormalization of the stiffness constants is ignored, the leading terms for the running d level and the running resonance width can be determined from

$$\frac{dE_d}{d\ln\xi} = (N-1)\frac{\Delta_0}{\pi}\left[\frac{\xi}{\xi_0}\right]^{-(2\epsilon_t-1)} ,$$

$$\frac{d\Delta}{d\ln\xi} = (1-2\epsilon_t)\Delta_0\left[\frac{\xi}{\xi_0}\right]^{-(2\epsilon_t-1)} , \tag{56}$$

where $\Delta_0 = \pi(y_t^0)^2/\xi_0$. This leads to

$$E_d(\xi) = E_d' + (N-1)\frac{\Delta_0}{\pi}\frac{1-(\xi/\xi_0)^{-(2\epsilon_t-1)}}{2\epsilon_t-1} ,$$

$$\Delta(\xi) = \Delta_0(\xi/\xi_0)^{-(2\epsilon_t-1)} , \tag{57}$$

from which we construct the invariant level and resonance width

$$E_d^* = E_d' + (N-1)\frac{\Delta_0}{\pi}\frac{1-(\Delta_0\xi_0)^{-(2\epsilon_t-1)/2(1-\epsilon_t)}}{2\epsilon_t-1} ,$$

$$\Delta^* = \Delta_0(\Delta_0\xi_0)^{(2\epsilon_t-1)/2(1-\epsilon_t)} . \tag{58}$$

In terms of these scaling invariants, the running d level and resonance width are given by

$$E_d(\xi) = E_d^* + (N-1)\frac{\Delta^*}{\pi}\frac{1-(\xi\Delta^*)^{-(2\epsilon_t-1)}}{2\epsilon_t-1} ,$$

$$\Delta(\xi) = \Delta^*(\xi\Delta^*)^{-(2\epsilon_t-1)} . \tag{59}$$

A logarithmic shift is recovered when $\epsilon_t = \epsilon_t^0 = \frac{1}{2}$ is used, corresponding to $V_1 = V_2 = 0$.

At low temperatures, the crossover between the various regimes can be determined from comparing the invariant d level E_d^* and the invariant resonance width Δ^*. The local-moment and empty-orbital regimes occur with $E_d^* \ll -\Delta^*$ and $E_d^* \gg \Delta^*$, respectively. For $|E_d^*| < \Delta^*$, the system is in the mixed-valence regime. This crossover behavior is illustrated in Fig. 4(a). Here we have used Eq. (7), so that the variation of E_d^* is described in terms of the chemical potential μ of the lattice model. At zero temperature, the mixed-valence crossover extends over a scale of $\sim \Delta^*$. This crossover can also be illustrated through the n vs μ curve, shown schematically in Fig. 5(a) and to be discussed further in Sec. V.

Finite temperature (or frequency) cuts off the scaling. As temperature is increased, both the running d level $E_d(T)$ and the running resonance width $\Delta(T)$ vary. The crossover temperature scale, separating the high-temperature mixed-valence regime from the low-temperature empty-orbital or local-moment regime, can
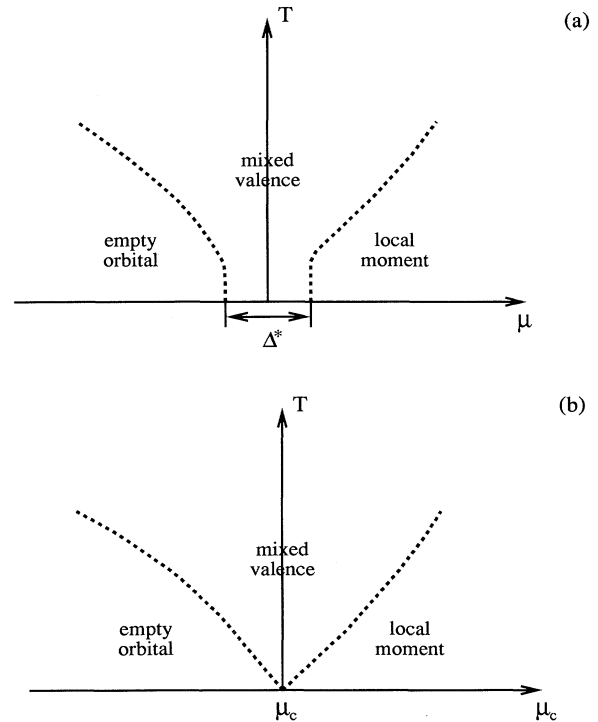

FIG. 4. Crossover diagram in terms of temperature (T) and chemical potential (μ) (a) for the strong-coupling case. The dashed lines correspond to the crossovers, and Δ^* is the renormalized resonance width and (b) for both the weak-coupling and the intermediate-coupling cases. Here μ_c labels the critical point.
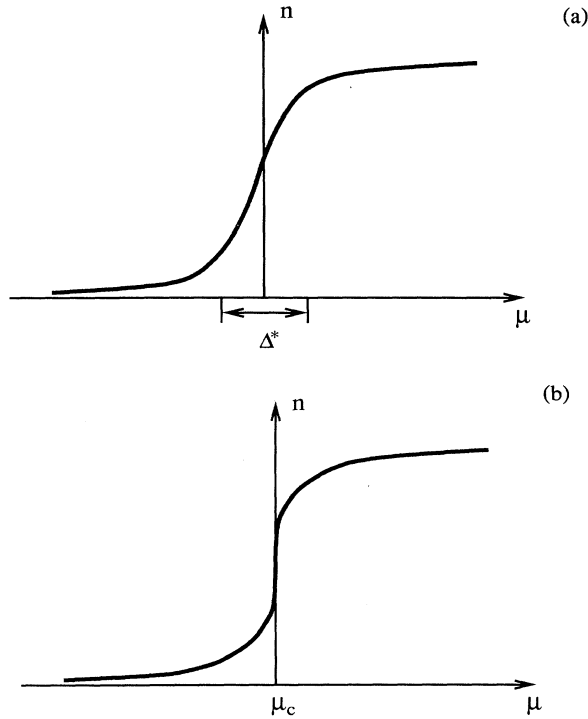
FIG. 5. Electron density (n) as a function of chemical potential (μ) (a) for the strong-coupling case and (b) for both the weak-coupling and the intermediate-coupling cases.

be determined from $E_d(T) = \max[T, \Delta(T)]$. This specifies the crossover lines—the dashed lines—in Fig. 4(a).[13] In the local-moment regime, there will be a further crossover at the scale of the Kondo temperature (not shown in the figure). In all these regimes, the low-energy behavior is described by the Fermi-liquid theory. The renormalized Fermi energy is given by the renormalized resonance width Δ^*.

D. Weak-coupling mixed-valence state

At the weak-coupling fixed points, the fugacities become smaller as we go down to lower energies. Therefore, the atomic expansion in terms of the running fugacities become more justified at lower energies. All the correlation functions can be derived from the RG procedure.

The running fugacities and d level can be derived from integrating the RG flow equations:

$$t(\omega) = t(\omega \xi_0)^{\epsilon_t^*} ,$$

$$V_{\frac{1}{2}}(\omega) = V_{\frac{1}{2}}(\omega \xi_0)^{\epsilon_j^*} , \qquad (60)$$

$$E_d(\omega) = E_d^* - \frac{A}{\xi_0}(\omega \xi_0)^{2\epsilon_t^* - 1} ,$$

where $A = (N-1)y_t^{02}/(2\epsilon_t^* - 1)$, and $E_d^* = E_d' + A/\xi_0$. In this case, the d-level shift due to the particle-hole asymmetry is small, since the hybridization is irrelevant.

The crossover diagram is given in Fig. 4(b). There

again exist local-moment, empty-orbital, and mixed-valence regimes. The important difference with the crossover diagram of the strong coupling phase [Fig. 4(a)] is that, in this case the renormalized resonance width Δ^* vanishes at zero temperature; A zero-temperature critical point occurs at $\mu = \mu_c$. This can also be shown through the n vs μ curve given in Fig. 5(b), where n is the total electron density.

To determine the finite-temperature crossovers between the different regimes, we define the running "resonance width" $\Delta(T)$ defined by

$$\Delta(T) = \pi y_t^2 T = \pi t^2 \xi_0 (T \xi_0)^{(2\epsilon_t^* - 1)} . \qquad (61)$$

The local-moment, empty-orbital, and the mixed-valence regimes occur when $E_d(T) \ll -\max[T, \Delta(T)]$, $E_d(T) \gg \max[T, \Delta(T)]$, and $|E_d(T)| < \max[T, \Delta(T)]$, respectively. This determines the crossover behavior illustrated in Figs. 4(b) and 5(b).

For $\sim(-A/\xi_0) < E_d^* < \sim A/\xi_0$, an additional crossover occurs at an energy scale T',

$$T' = \frac{1}{\xi_0} \left[\frac{|E_d^*|\xi_0}{A} \right]^{1/(2\epsilon_t^* - 1)} , \qquad (62)$$

which is determined from $|E_d(T')| \sim \Delta(T')$. The system is in the critical regime at temperatures higher than T', since here it is essentially an $E_d(T) = 0$ problem, with a temperature dependent resonance width, which is smaller than the temperature. In particular, at $E_d^* = 0$, i.e., $\mu = \mu_c$, this mixed-valence critical regime persists all the way down to zero temperature. The mixed-valence state corresponds to a massless critical point.

The mixed-valence phase here is characteristically different from the strong-coupling mixed-valence phase. The irrelevant hybridization causes the running resonance width to be always smaller than the scale, $\Delta(\omega) < \omega$. Local correlation functions in the mixed valence regime can be calculated through the RG procedure.[32]

Here we focus on the local Green's function, which is a 2×2 matrix for each spin component:

$$G = \begin{bmatrix} G_{cc} & G_{cd} \\ G_{dc} & G_{dd} \end{bmatrix} . \qquad (63)$$

The details of the RG calculation for the renormalization of the exponents can be found in Appendix C. The results are as follows. G_{dc} and G_{dd} exhibit infrared divergences, and have the following low-energy behavior:

$$G_{dc}(\omega) \sim \omega^{-1+\alpha} ,$$
$$G_{dd}(\omega) \sim \omega^{-1+\beta} . \qquad (64)$$

Here the exponents are, to leading order, as follows:

$$\alpha = -(\delta_1^* + \delta_2^*)/\pi + [(\delta_1^* + \delta_2^*)/\pi]^2 + (N-1)(\delta_1^*/\pi)^2 ,$$
$$\beta = [(\delta_1^* + \delta_2^*)/\pi]^2 + (N-1)(\delta_1^*/\pi)^2 , \qquad (65)$$

where $\delta_{1,2}^*$ are the renormalized phase shifts determined from Eq. (51). The algebraic divergences in G_{dc} and G_{dd} reflect the fact that, both the impurity spin and charge

degrees of the freedom are not quenched.

On the other hand, the local c-electron Green's function G_{cc} does not show infrared divergences. Formally, creating a local c electron does not create any kink in the path integral representation. Hence, G_{cc} is not renormalized from its fixed point form. At the mixed-valence

point, G_{cc} has a long-time $1/\tau$ behavior. The absence of infrared divergences in the electron bath spectral function will be used in Sec. V D to argue that our results derived using a Lorentzian density of states can be applied to the case of generic density of states as well.

E. Intermediate-coupling mixed-valence state

In this case, the RG equations yield an initially decreasing charge fugacity y_t and an initially increasing spin fugacity y_j. When y_j grows to order unity, the flow equations would indicate that y_t starts to grow. However, this is beyond the regime of validity for the perturbative RG.

To understand qualitatively the nature of the fixed point, we analyze the model in the limit that the antiferromagnetic exchange V_2 is much larger than the conduction electron bandwidth, while the hybridization t is much smaller than the bandwidth. This serves as an effective Hamiltonian that the original Hamiltonian renormalizes to at an intermediate scale.

$$\tilde{H}_{\text{eff}} = V_2 \sum_{\sigma,\sigma'} d_\sigma^\dagger d_{\sigma'} c_{0,\sigma'}^\dagger c_{0,\sigma} + V_1 \sum_{\sigma,\sigma'} d_\sigma^\dagger d_\sigma c_{0,\sigma'}^\dagger c_{0,\sigma'} + \epsilon_d' \sum_\sigma d_\sigma^\dagger d_\sigma + \frac{U}{2} \sum_i \sum_{\sigma \neq \sigma'} d_{i\sigma}^\dagger d_{i\sigma} d_{i\sigma'}^\dagger d_{i\sigma'}$$

$$+ \sum_\sigma t(d_\sigma^\dagger c_{0,\sigma} + \text{H.c.}) + \sum_{i_1,\sigma} t_1(c_{1,\sigma}^\dagger c_{0,\sigma} + \text{H.c.}) + \sum_{\langle i,j \neq 0 \rangle} t_{ij}(c_{i,\sigma}^\dagger c_{j,\sigma} + \text{H.c.}) \ . \tag{66}$$

Here $c_{1,\sigma}^\dagger$ creates effective neighboring states, which are coupled to the conduction-electron state at the impurity site that $c_{0,\sigma}^\dagger$ creates. We consider $N=2$ for simplicity. The parameters are such that $V_2 \gg V_1$, $t_1 \gg t$, and $U = \infty$.

To order $O(t_1/V_2, t/V_2)$, diagonalizing the V_2 coupling first leads to singlet and triplet subsectors within the $n_d = 1$ sector. And the triplet sector locates at high energies. The mixed-valence condition is satisfied at an ϵ_d' such that the singlet sector and the $n_d = 0$ sector are (nearly) degenerate. We can now integrate out the high-energy states. This leads to the following effective Hamiltonian for the low-energy sectors,

$$H_{\text{eff}} = \epsilon_s(s^\dagger s - e^\dagger e) + \sum_k \tilde{\epsilon}_k \tilde{c}_{k,\sigma}^\dagger \tilde{c}_{k,\sigma} + \sum_{k,k',\sigma} [t_{k,k'}' s^\dagger e \tilde{c}_{k,\sigma} \tilde{c}_{k,-\sigma} \text{sgn}(\sigma) + \text{H.c.}] + \sum_{k,k',\sigma} V_{k,k'}'(s^\dagger s - e^\dagger e)\tilde{c}_{k,\sigma}^\dagger \tilde{c}_{k,\sigma} \ . \tag{67}$$

Here $s^\dagger$ and $e^\dagger$ create the local singlet and the local empty state, respectively, while $\tilde{c}_{k,\sigma}^\dagger$ creates conduction-electron scattering states. The effective interaction and the effective "hybridization" are given as follows:

$$V_{k,k'}' \sim \frac{2V_1}{(V_2 - V_1)(V_2 + V_1)} t_1^2 \ ,$$

$$t_{k,k'}' \sim \frac{1}{2} t \ . \tag{68}$$

Given that t is small, and $V_s' < 0$, the effective hybridization is *marginally irrelevant*. Therefore, the spin and charge sectors are indeed decoupled asympotically.

The crossover diagram is also given qualitatively by Fig. 4(b), except for the local moment regime in which the spin degrees of freedom is eventually quenched through the Kondo process. The n vs μ curve at zero temperature is again qualitatively given by Fig. 5(b).

For the mixed-valence regime, the spectral functions have the form of a convolution between the resonance in the spin sector and the algebraic term in the charge sector, and therefore also exhibit an algebraic behavior at low energies. The exponents can be determined from the effective charge stiffness constants, renormalized (further from ϵ_t^*) due to the screening of the free-spin-kink plasma. This further renormalization can be analyzed in detail by following the scaling trajectory and using Eq. (67), in the same spirit as the analysis of the hexatic phase

using the Debye-Hückel approximation.[35] In particular, the exponent is universal when the critical line separating the intermediate coupling and the strong-coupling states, i.e., the dashed line in Fig. 2, is approached.

V. NON-FERMI-LIQUID AND FERMI-LIQUID PHASES OF THE EXTENDED HUBBARD MODEL

In this section, we establish the implications of the results of the associated impurity problem in the preceding two sections on the phases in the extended Hubbard model. We show that the phases corresponding to the weak-coupling and intermediate-coupling mixed-valence states are metallic non-Fermi-liquid phases. They have vanishing quasiparticle residue, algebraic local correlation functions, and asymptotically separated charge and spin excitations. The phase corresponding to the strong-coupling mixed-valence state is a usual Fermi liquid.

A. Metallic non-Fermi-liquid: Weak-coupling and intermediate-coupling phases

Consider first the phase corresponding to the weak-coupling mixed-valence state. We first establish that the critical chemical potential μ_c, at which the mixed-valence state persists to zero temperature, corresponds to *a range of electron densities.*

The local correlation functions of the extended Hub-

bard model in infinite dimensions are given by the impurity problem. In particular, the occupation numbers in the lattice, for a given chemical potential, can be obtained from the local Green's functions of the corresponding impurity model. Therefore, our analyses in Secs. II C and IV D establish that, at zero-temperature, n_d (and also $n = n_d + n_c$) are discontinuous functions of the chemical potential: $n_d \approx 1 - O(t^2)$ for $\mu > \mu_c$, while $n_d \approx O(t^2)$ for $\mu < \mu_c$. At finite temperatures, the discontinuity is smoothed out and changes into a fast crossover. Here we take $\mu = \mu_c$, which again corresponds to a *finite range* of densities in the lattice model.

It is remarkable that the fact that our impurity model is associated to a lattice problem forces the impurity model to be exactly at criticality, with a larger symmetry than we would have naively expected. The essential point is that in order for an *incoherent state* to be metallic, it is necessary to allow for charge transfer between the local degrees of freedom and the bath. This can only happen if the local charge degree of freedom is in equilibrium with the conduction electron bath. This requires the heavy level to be at the chemical potential.

To determine the excitation spectrum of the system, we consider the lattice Green's function

$$G(\mathbf{k},\tau) = \begin{bmatrix} G_{cc}(\mathbf{k},\tau) & G_{cd}(\mathbf{k},\tau) \\ G_{dc}(\mathbf{k},\tau) & G_{dd}(\mathbf{k},\tau) \end{bmatrix} = \begin{bmatrix} -\langle Tc_{\mathbf{k}}(\tau)c_{\mathbf{k}}^{\dagger}(0)\rangle & -\langle Tc_{\mathbf{k}}(\tau)d_{\mathbf{k}}^{\dagger}(0)\rangle \\ -\langle Td_{\mathbf{k}}(\tau)c_{\mathbf{k}}^{\dagger}(0)\rangle & -\langle Td_{\mathbf{k}}(\tau)d_{\mathbf{k}}^{\dagger}(0)\rangle \end{bmatrix} , \tag{69}$$

which can be determined from the Dyson equation for the lattice model

$$G(\mathbf{k},i\omega_n) = \begin{bmatrix} i\omega_n + \mu - \epsilon_{\mathbf{k}} - \Sigma_{cc}(i\omega_n) & t - \Sigma_{cd}(i\omega_n) \\ t - \Sigma_{dc}(i\omega_n) & i\omega_n + \mu - \epsilon_d^0 - \Sigma_{dd}(i\omega_n) \end{bmatrix}^{-1} , \tag{70}$$

where the momentum-independent self-energy can be calculated directly from the local Green's functions of the impurity model

$$\Sigma(i\omega_n) = \begin{bmatrix} \Sigma_{cc}(i\omega_n) & \Sigma_{cd}(i\omega_n) \\ \Sigma_{dc}(i\omega_n) & \Sigma_{dd}(i\omega_n) \end{bmatrix} = \begin{bmatrix} (G_0^{-1})_{cc}(i\omega_n) & (G_0^{-1})_{cd}(i\omega_n) \\ (G_0^{-1})_{dc}(i\omega_n) & (G_0^{-1})_{dd}(i\omega_n) \end{bmatrix} - \begin{bmatrix} G_{cc}(i\omega_n) & G_{cd}(i\omega_n) \\ G_{dc}(i\omega_n) & G_{dd}(i\omega_n) \end{bmatrix}^{-1} . \tag{71}$$

This leads to, for $N > 1$, the following form for the frequency dependence of the self-energies:

$$\Sigma_{cc}(\omega) \sim (\omega)^{\gamma_{cc}} ,$$

$$\Sigma_{dd}(\omega) \sim (\omega)^{\gamma_{dd}} , \tag{72}$$

$$\Sigma_{dc}(\omega) \sim (\omega)^{\gamma_{dc}} .$$

Here the exponents $\gamma_{cc} = 2\epsilon_t^* - 2$, $\gamma_{dd} = 1 - \alpha$, and $\gamma_{dc} = 2\epsilon_t^* + \beta - 1$, where α and β are the exponents associated with G_{dd} and G_{dc} given in Eq. (65).

The form of the self-energies given in Eq. (72) destroys the quasiparticle poles. Therefore, the quasiparticle residue vanishes; all the single-particle excitations are incoherent.

We now turn to various physical correlation functions. Since both the impurity spin and the charge couplings are irrelevant, we expect that the multiparticle correlation functions in both impurity spin and charge channels show power-law behavior. The spin and charge-correlation functions are generally renormalized differently. The precise values of the exponents can be derived using RG as discussed in Appendix C. For example,

$$\langle d_{\sigma}^{\dagger}d_{\sigma'}(\tau)d_{\sigma'}^{\dagger}d_{\sigma}(0)\rangle \sim (\tau)^{-\alpha_1} ,$$

$$\langle d_{\sigma}^{\dagger}c_{\sigma'}(\tau)c_{\sigma'}^{\dagger}d_{\sigma}(0)\rangle \sim (\tau)^{-\alpha_2} , \tag{73}$$

$$\langle d_{\sigma}^{\dagger}c_{\sigma'}^{\dagger}(\tau)c_{\sigma'}d_{\sigma}(0)\rangle \sim (\tau)^{-\alpha_3} ,$$

where to leading order

$$\alpha_1 = 2\epsilon_j^*(1 - \delta_{\sigma,\sigma'}) ,$$

$$\alpha_2 = 2\epsilon_t^*\delta_{\sigma,\sigma'} + 2\epsilon_{tj}^*(1 - \delta_{\sigma,\sigma'}) , \tag{74}$$

$$\alpha_3 = 2\epsilon_t^* \left[-\frac{\delta_1^*}{\pi}, -\frac{\delta_2^*}{\pi} \right]\delta_{\sigma,\sigma'}$$

$$+ 2\epsilon_{tj}^* \left[-\frac{\delta_1^*}{\pi}, -\frac{\delta_2^*}{\pi} \right](1 - \delta_{\sigma,\sigma'})$$

in which

$$\epsilon_{tj}^* \left[\frac{\delta_1^*}{\pi}, \frac{\delta_2^*}{\pi} \right] = \left[\left[1 - \frac{\delta_1^*}{\pi} \right]^2 + \left[\frac{\delta_1^*}{\pi} + \frac{\delta_2^*}{\pi} \right]^2 \right.$$

$$\left. + (N-2) \left[\frac{\delta_1^*}{\pi} \right]^2 \right] \Big/ 2 .$$

These exponents correspond to a divergent $d^{\dagger}c^{\dagger}$ pairing susceptibility and vanishing excitonic and d-electron correlation functions at low energies. The divergent pairing susceptibility signals a superconducting instability at a finite temperature T_c, with an anomalous normal state described by the non-Fermi-liquid state. We will comment on this further in Sec. VI.

We now turn to the intermediate-coupling phase. A critical chemical potential μ_c also exists due to the irrelevant hybridization, as was established in Sec. IV E. It again corresponds to a *finite range* of densities in the lat-

tice model, at which the mixed valence behavior persists to zero temperature.

Since the exchange coupling is relevant, a resonance forms in the spin channel below the corresponding coherence energy. Therefore, spin excitations form quasiparticles, which are expected to have Fermi-surface features. The local spin susceptibility is regular. On the other hand, the local charge susceptibility retains the algebraic behavior. The excitonic correlation function still vanishes in the zero-frequency limit, while the superconducting $d^\dagger c^\dagger$ susceptibility still diverges at low frequencies algebraically: the system is again expected to be a superconductor with an anomalous normal state.

To summarize, the non-Fermi-liquid phases characterize incoherent metals with vanishing quasiparticle residue, self-similar local correlation functions, and asymptotically decoupled charge and spin excitations. In addition, they occur over a range of electron densities due to the pinning effect.

B. Fermi-liquid phase

We now turn to the region where the hybridization is relevant. The system then flows away from the zero-fugacity fixed points. The new fixed point is beyond the reach of the perturbative RG. The nature of the fixed point can be studied by other approaches describing the strong-coupling phases. One approach is the large-N limit of the model with fixed finite values of V_1 and V_2.[43,44]

In the large-N mean-field theory applied directly to the lattice model (1), the renormalized hybridization never vanishes, and the density is a continuous function of the chemical potential. The d-electron spectral function exhibits a coherent Abrikosov-Suhl resonance. Low-energy excitations are coherent and are composed of conduction electrons and heavy electrons with finite hybridization. The system is a Fermi liquid.

That the large-N limit forces the system to be a Fermi liquid can be easily understood from our scaling equations (49). When the large-N limit is taken, with fixed finite values of V_1 and V_2, the associated phase shifts given in Eqs. (27) and (28) vanish. Hence, the anomalous dimensions of the spin and charge flippings, defined in Eqs. (48) and (27), fall in the basin of attraction of the strong-coupling fixed points. Physically, the excitonic and orthogonality contributions are suppressed by a factor of $1/N$.

C. Qualitative phase diagram
of the extended Hubbard model

The qualitative phase diagram, in terms of the interaction strength and electron density, is summarized in Fig. 6. Figure 6(a) corresponds to varying the interaction strength (in the $\epsilon_t - \epsilon_j$ plane in Fig. 2) as that characterized in Fig. 3(a). For the interaction strength such that ϵ_1 is above the threshold value ϵ_c given in Fig. 3(a), and over a range of electron density given by the solid-line shaded region, a mixed-valence metallic non-Fermi-liquid state occurs down to lowest temperatures (see, however, the discussion about long-range ordering in Sec. VI).

This range of density corresponds to the critical chemical potential μ_c in Figs. 4(b) and 5(b). For electron densities outside this range, within the dashed-line shaded region, non-Fermi-liquid behavior occurs above a crossover temperature, shown in Fig. 4(b). The non-Fermi-liquid state is characterized by incoherent charge and spin excitations, which are asymptotically decoupled.

For interaction strength such that ϵ_1 is below the threshold value ϵ_c, the system is a Fermi liquid. It corresponds to the strong-coupling mixed-valence state of the associated generalized Anderson model. Near the threshold interaction strength, the Fermi energy is given by Eq. (55) with the exponent $\eta = \frac{1}{2}$.

In Fig. 6(b), we vary the interaction strength as that characterized in Fig. 3(b). For interaction strength such that ϵ_2 is above the threshold value ϵ_{c2} in Fig. 3(b), a (weak-coupling mixed-valence) metallic non-Fermi-liquid phase again occurs down to zero temperature over a range of electron density within the solid-horizontal-line
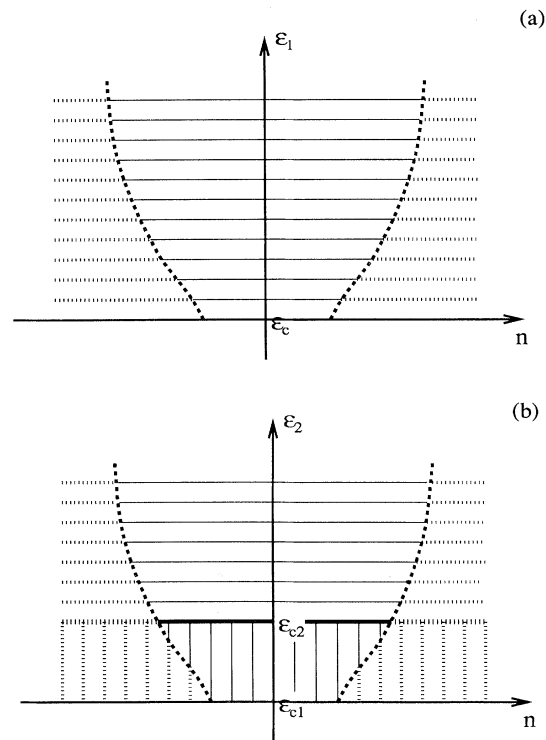

FIG. 6. Schematic interaction-density phase diagram for two ways of varying the interactions. Here ϵ_1 and ϵ_2 are the same as those in Fig. 3. (a) For ϵ_1 above ϵ_c, non-Fermi-liquid phase with both charge and spin excitations incoherent occurs till zero temperature within the solid-line shaded density range, and above a crossover temperature within the dashed-line shaded density range. The Fermi-liquid phase occurs otherwise. (b) For ϵ_2 above ϵ_{c1}, the non-Fermi-liquid phase of (a) occurs. For ϵ_2 between ϵ_{c1} and ϵ_{c2}, the non-Fermi-liquid phase with incoherent charge excitations but coherent spin excitations occurs till zero temperature within the solid-vertical-line shaded density range, and above a crossover temperature within dashed-vertical-line shaded density range. The Fermi-liquid phase occurs otherwise.

shaded region, and above a crossover temperature for electron densities within the dashed-horizontal-line shaded region. The non-Fermi-liquid state is the same as that in Fig. 6(a).

For interaction strength such that ϵ_2 is between ϵ_{c1} and ϵ_{c2} of Fig. 3(b), and over a range of electron density given by the solid-vertical-line shaded region, an (intermediate-coupling mixed-valence) metallic non-Fermi-liquid phase occurs down to lowest temperatures. For electron densities within the dashed-vertical-line shaded region, the non-Fermi-liquid behavior occurs above a crossover temperature given in Fig. 4(b). The non-Fermi-liquid state is characterized by coherent spin excitations and incoherent charge excitations, which also decouple asymptotically at low energies. The spin coherence energy near ϵ_{c1} is given by Eq. (55) with the exponent $\eta = 1$.

Finally, for interaction strength such that ϵ_2 is below the threshold value ϵ_{c1}, the system is a Fermi liquid, corresponding to the strong-coupling state.

D. Dependence on the form of the density of states

Thus far, we have focused on the extended Hubbard model with a Lorentzian density of states. The non-Fermi-liquid phases occur due to the persistance of asymptotically degenerate states at the Fermi level. This occurs because the quantum hopping amplitude (the hybridization), which mixes these degenerate states is irrelevant. These couplings are irrelevant because of the slow relaxation of the electron bath to the hopping between different local charge states. Such a large reaction exists whenever there are nonzero density of states of the electron bath at the Fermi level. In the Lorentzian case, there is always a finite density of states for the bath electron.

To establish the generality of our results, we consider the extended Hubbard model defined on the Bethe lattice with infinite connectivity. In this case, the bare density of states is bounded.[45,10] The Weiss field G_0^{-1}, which is a 2×2 matrix in our case, can be explicitly related to the full Green's function,

$$G_0^{-1}(i\omega_n) = g_0^{-1}(i\omega_n) - \sum_{ij} t_{0i} G_{ij} t_{j0} , \qquad (75)$$

where g_0^{-1} is the inverse propagator of the corresponding noninteracting problem. More explicitly,

$$(G_0^{-1})_{dd} = i\omega_n + \mu - E_d^0 ,$$

$$(G_0^{-1})_{cd} = t , \qquad (76)$$

$$(G_0^{-1})_{cc} = i\omega_n + \mu - (t_{cc})^2 G_{cc} .$$

Such a relation demonstrates that when the renormalized c-electron density of states is nonzero at the chemical potential, the Weiss field $(G_0^{-1})_{cc}$ will have a nonzero imaginary part. When the hybridization t is small, the c electron acts as the electron bath that the local d-electron degrees of freedom couple to. Since the c-electron Green's function does not show infrared divergences, as discussed in Secs. IV D and IV C, the local Green's func-

tion of the electron bath has the long-time asymptotic $1/\tau$ behavior. This establishes that a finite density of states for the electron bath at the Fermi level is indeed self-consistent. This finite density of states can be effectively modeled as the inverse Lorentzian width.[46]

Therefore, our results, which are explicitly derived for the extended Hubbard model with a Lorentzian density of states, are expected to reflect qualitatively the physics of the extended Hubbard model away from half filling. At the quantitative level, one has to determine the charge and spin stiffness constants ϵ_t and ϵ_j, used in constructing the phase diagram in Fig. 2, through integrating out nonuniversal high-energy dynamics. The phase diagram will be altered correspondingly.

Finally, within the model with zero direct d-electron hopping, only $(G_0^{-1})_{cc}$ has a nontrivial form. Hence, direct d-electron hopping effects are not generated. How new energy scales might be generated from an explicit direct d-electron hopping term is an important issue to be further studied.

VI. CONCLUSION

We have carried out a detailed study of an extended Hubbard model in infinite dimensions, where the model reduces to a generalized asymmetric Anderson problem in a self-consistent medium. Within the associated impurity problem, we carried out a systematic renormalization-group analysis, and identified three kinds of mixed-valence behavior. Each of these states is associated with a distinctive flow of spin and charge couplings. The usual strong-coupling mixed-valence state has spin and charge couplings both relevant, the weak-coupling mixed-valence state has spin and charge couplings both irrelevant, and the intermediate-coupling mixed-valence state has a relevant spin coupling and irrelevant charge coupling. The strong-coupling state corresponds to a Fermi-liquid phase of the extended Hubbard model, while both the weak-coupling and the intermediate-coupling mixed-valence states describe metallic non-Fermi-liquid phases of the extended Hubbard model.

The non-Fermi-liquid phases are metallic states with incoherent charge excitations. Within these incoherent metallic states, the local charge modes are necessarily close to the Fermi level for charge transport to occur. Such a pinning effect makes the non-Fermi-liquid phases to occur over *a range of electron densities*. Hence, no fine tuning of parameters is necessary. The pinning of the chemical potential leads to an infinite compressibility at zero temperature: there is a jump in the n vs μ curve, as shown in Fig. 5(b). It is interesting to note that an infinite compressibility has been demonstrated in the numerical studies of the Hubbard model in the limit of small dopings away from half filling.[47]

The non-Fermi-liquid phases have vanishing quasiparticle residue: all excitations are incoherent. In addition, charge and spin excitations decouple asymptotically at low energies. Finally, certain local correlation functions show algebraic behavior, reflecting the self-similar nature of these incoherent metallic states. These are the local correlations in both the charge and spin channels in the

weak-coupling phase, and in charge but not spin channel in the intermediate coupling phase. These properties have striking analogies to the Luttinger liquid in one dimension.[4,3]

The intermediate-coupling phase that we identify has coherent spin excitations and incoherent charge excitations. In connection with the possible realization of such a phase in strongly correlated electron systems, we note that, within the normal state of the high-T_c copper oxides, the low-energy spin dynamics are well described by renormalized quasiparticles with a Fermi surface satisfying the Luttinger theorem, while the charge dynamics appear to be more anomalous.[48] We will discuss physical properties of our intermediate phase in more detail elsewhere.

We stress that at the end one ought to be able to express our results, derived using a local method, in a language that would make contact with perturbative calculations in the interactions. When this is done we may be able to identify some similarities between our results and those derived from other methods. This will also allow us to extend our results to models at finite dimensions. In this regard, the Fermi-liquid phase is described in terms of the boson "condensed" phase within the slave-boson formalism: the hybridization renormalization is determined by the quasicondensate of the slave boson, and the d level renormalization is given by the mean-field value of a Lagrangian multiplier enforcing the no-double-occupancy constraint.[43] Our intermediate-coupling incoherent metallic state has similarities with the boson noncondensed phase,[49] which also has coherent spin excitation ("spinon") and incoherent charge excitation ("holon"). From our local treatment, the characteristics of an incoherent metallic state lie in its self-similar nature, a problem without scale. In both treatments of these incoherent metallic states, the local gauge invariance, which is broken by the coherent hopping is finally restored.

We now comment on several aspects of our results, which are important to address in order to apply our results to finite dimensions as well as to more general models.

In general, the limit of infinite dimensions separates the single particle and collective excitations. As a result, when the system undergoes an ordering instability, the one-particle property does not show precursor effect; the feedback of the long-range order over the single-particle properties is down by powers of $1/d$. Within the incoherent metallic phases, there exist asymptotically degenerate local configurations, which are manifested in the algebraic low-energy behavior in various local correlation functions. In finite dimensions, the coupling of the long-range order on the local physics modifies the local effective action at temperatures below the onset temperature T_c, and has the effect of cutting off the power-law singularities. In our incoherent metallic states, the most divergent local susceptibility is a pairing susceptibility. Therefore, the instability is expected to be in the superconducting channel. Our incoherent metallic states are then expected to be relevant at temperatures $T_c \ll T \ll \omega_c$ in the same sense that the paramagnetic

Mott insulating phase is well defined for $T_N \ll T \ll \epsilon_F$ (T_N being the Néel temperature).

Within the extended Hubbard model in infinite dimensions with a Lorentzian density of states, the weak-coupling incoherent metallic state occurs over a range of attractive density-density interactions and ferromagnetic spin interactions, while the intermediate-coupling incoherent metallic state occurs over a range of attractive charge interactions and antiferromagnetic spin interactions. We emphasize that a Lorentzian form for the density of states suppresses the high-energy dynamics, enforcing the system to be always in the scaling regime. In the generic case, the electron bath will be in the universal regime only within a narrow energy range around the Fermi level. The high-energy dynamics have to be integrated out before the renormalization group results can apply. Our results here, derived for an extended Hubbard model with a Lorentzian density of states, give the classification of the universality classes for a general $N+1$ local configuration problem. To determine the basin of attraction of the various phases, one has to first integrate out the high-energy dynamics beyond the scaling regime. Such a procedure makes it possible that realistic Hamiltonians with all repulsive atomic interactions fall in the basin of attraction of the non-Fermi-liquid phases.[50] Within generic models, the basin of attraction of nontrivial phases can be determined numerically.

We conclude with a note on the methodology implications of our analysis. The general renormalization-group scheme developed here opens a local view for strongly correlated electron systems. The universality classes of a correlated electron system can be determined by a small number of atomic configurations coupled to an electron bath, which can be treated through the general atomic expansion plus the renormalization-group procedure we outlined here. The specifications of the phase diagram, on the other hand, involve integrating out nonuniversal high-energy dynamics, which falls in the domain of quantum chemistry.[50]

APPENDIX A: BOSONIZATION AND THE LEVEL SHIFT

In this appendix, we summarize the bosonization procedure[39,3] relevant to our discussion. We also discuss the shift in the atomic levels that should be incorporated in carrying out the bosonization.

Consider the projected Hamiltonian given in Eq. (15),

$$H_\alpha = E_\alpha + \sum_\sigma V_\alpha^\sigma c_\sigma^\dagger c_\sigma + H_c , \tag{A1}$$

where

$$H_c = \sum_{k,\sigma} E_k c_{k\sigma}^\dagger c_{k\sigma} . \tag{A2}$$

For the asymptotic behavior, as long as the density of states of the conduction electron is finite, a bosonization scheme can be used. For the purpose of studying an impurity problem, we need to consider only the S-wave component of the conduction electrons. We label the radial dimension by x, which is extended to the negative half axis.

The Tomonaga bosons are defined as follows:

$$b_{q,\sigma}^\dagger = i\sqrt{2\pi/qL} \sum_k c_{k+q,\sigma}^\dagger c_{k,\sigma} \ ,$$
$$b_{q,\sigma} = -i\sqrt{2\pi/qL} \sum_k c_{k,\sigma}^\dagger c_{k+q,\sigma} \ ,$$

(A3)

where $q > 0$, and L is the size of the radial dimension.

The free-electron Hamiltonian has the following form in terms of the Tomonaga bosons:

$$H_c = \sum_{q,\sigma} v_F q b_{q,\sigma}^\dagger b_{q,\sigma} \ ,$$

(A4)

where the boson dispersion is determined by $v_F = 1/\rho_0$, the inverse of the density of states at the Fermi level.

The conduction electron operator has the following form:

$$c_\sigma(x) = \frac{1}{\sqrt{2\pi a}} e^{-i\Phi_\sigma(x)} \ ,$$

(A5)

where

$$\Phi_\sigma(x) = \sum_q \sqrt{2\pi/qL} (b_q^\dagger e^{-iqx} + b_q e^{iqx}) \ .$$

(A6)

The electron density, $\rho_\sigma(x) = c_\sigma^\dagger c_\sigma$, is related to the Φ_σ field as follows:

$$\rho_\sigma(x) = \frac{d\Phi_\sigma}{dx} \ .$$

(A7)

Therefore, the potential term can be represented as follows:

$$V_\alpha^\sigma c_\sigma^\dagger c_\sigma = \frac{\delta_\alpha^\sigma}{\pi\rho_0} \left[\frac{d\Phi_\sigma}{dx} \right]_{x=0} \ .$$

(A8)

We use the prescription that all quantities in the bosonization representation correspond to the normal ordered quantities. In so doing, a Hartree-like shift in energy has to be incorporated separately. The exact form of such a level shift was discussed in detail for the spinless case in Ref. 26. It can be easily generalized to arbitrary

spin degeneracy N, leading to

$$\Delta E_\alpha = \frac{1}{\beta} \sum_\sigma \sum_n \{\ln(g_0^{-1}) - \ln(g_0^{-1} - V_\alpha^\sigma)\} e^{i\omega_n 0^\dagger} \ ,$$

(A9)

where $g_0(i\omega_n) = \sum_k 1/(i\omega_n + \mu - \epsilon_k)$. The linear in V term in the above shift ΔE_α is given by the $q=0$ component of the Tomonaga boson.

Such a shift can be captured by expressing H_α in the bosonization form,

$$H_\alpha = H_c + E_\alpha' + \sum_\gamma \frac{\delta_\alpha^\gamma}{\pi\rho_0} \left[\frac{d\Phi_\gamma}{dx} \right]_{x=0} \ ,$$

(A10)

where $E_\alpha' = E_\alpha + \Delta E_\alpha$.

APPENDIX B: RENORMALIZATION-GROUP EQUATIONS

In this appendix, we present the details of the derivation for the RG equations, which will be written in the general form, for M arbitrary local configurations $|\alpha\rangle$.

The RG equations describe the flow of the dimensionless couplings as the bandwidth $1/\xi$ is reduced. The RG charges are the fugacities $y_{\alpha\beta}$, the stiffness constants $-K(\alpha,\beta)$, and the symmetry-breaking fields h_α. They satisfy $y_{\alpha\alpha} = 0$, $K(\alpha,\alpha) = 0$, and $\sum_\alpha h_\alpha = 0$. These relations are preserved in the renormalization process.

Integrating out the degrees of freedom in the range $(\xi, \xi + d\xi)$ leads to three kinds of renormalization contributions. One contribution arises from rescaling the old cutoff ξ by the new one $\xi' = \xi + d\xi$ in Eqs. (42)–(44). This amounts to a renormalization of the fugacities and the fields,

$$y_{\alpha_{i+1},\alpha_i} \to y_{\alpha_{i+1},\alpha_i} [1 + (d\ln\xi)(1 + K_{\alpha_{i+1},\alpha_i})] \ ,$$
$$h_{\alpha_i} \to h_{\alpha_i} (1 + d\ln\xi) \ .$$

(B1)

The other contributions arise from the change in the integration range in the partition function, Eq. (42). The dominant renormalization arises from integrating out kink pairs whose separation falls in the range $(\xi, \xi + d\xi)$. There are two kinds of contributions in this category.

The contributions from integrating out non-neutral pairs, i.e., pairs with the final state of the second kink different from the initial state of the first kink, amounts to a change in the fugacities:

$$y_{\alpha_{i+1},\alpha_i} \to y_{\alpha_{i+1},\alpha_i} + (d\ln\xi) \sum_\gamma y_{\alpha_{i+1},\gamma} y_{\gamma,\alpha_i} e^{(h_{\alpha_{i+1}} + h_{\alpha_i} - 2h_\gamma)/2}$$

(B2)

for $\alpha_{i+1} \neq \alpha_i$.

On the other hand, integrating out neutral pairs leads to a renormalization of the stiffness constants,

$$K_{\alpha_{i+1},\alpha_i} \to K_{\alpha_{i+1},\alpha_i} - d(\ln\xi) \sum_\gamma y_{\alpha_{i+1},\gamma}^2 e^{h_{\alpha_{i+1}} - h_\gamma} (K_{\alpha_{i+1},\alpha_i} + K_{\alpha_{i+1},\gamma} - K_{\alpha_i,\gamma})$$

$$- d(\ln\xi) \sum_\gamma y_{\alpha_i,\gamma}^2 e^{h_{\alpha_i} - h_\gamma} (K_{\alpha_{i+1},\alpha_i} + K_{\alpha_i,\gamma} - K_{\alpha_{i+1},\gamma})$$

(B3)

as well as a renormalization in the field and in the free energy,

$$h_{\alpha_i} \to h_{\alpha_i} - d(\ln\xi) \left[\sum_\gamma y_{\alpha_i,\gamma}^2 e^{h_{\alpha_i} - h_\gamma} - \frac{1}{M} \sum_{\gamma_1,\gamma_2} y_{\gamma_1,\gamma_2} e^{h_{\gamma_1} - h_{\gamma_2}} \right] ,$$

$$F\xi \to F\xi - d(\ln\xi) \frac{1}{M} \sum_{\gamma_1,\gamma_2} y_{\gamma_1,\gamma_2}^2 e^{h_{\gamma_1} - h_{\gamma_2}} .$$

(B4)

Here the separation into the field renormalization and free-energy renormalization is unambiguously specified by requiring that $\sum_\alpha h_\alpha = 0$ be preserved in the process of renormalization.

Collecting all these terms, we derive the following general form of the RG equations.

$$\frac{dy_{\alpha,\beta}}{d\ln\xi} = [1 + K(\alpha,\beta)]y_{\alpha,\beta} + \sum_\gamma y_{\alpha,\gamma} y_{\gamma,\beta} e^{(h_\alpha + h_\beta - 2h_\gamma)/2} ,$$

$$\frac{dK(\alpha,\beta)}{d\ln\xi} = -\sum_\gamma y_{\alpha,\gamma}^2 e^{h_\alpha - h_\gamma} [K(\alpha,\beta) + K(\alpha,\gamma) - K(\beta,\gamma)] - \sum_\gamma y_{\beta,\gamma}^2 e^{h_\beta - h_\gamma} [K(\alpha,\beta) + K(\beta,\gamma) - K(\alpha,\gamma)] ,$$

$$\frac{dh_\alpha}{d\ln\xi} = h_\alpha - \sum_\gamma y_{\alpha,\gamma}^2 e^{h_\alpha - h_\gamma} + \frac{1}{M} \sum_{\alpha,\beta} y_{\alpha,\beta}^2 e^{h_\alpha - h_\beta} ,$$

$$\frac{dF\xi}{d\ln\xi} = F\xi - \frac{1}{M} \sum_{\alpha,\beta} y_{\alpha,\beta}^2 e^{h_\alpha - h_\beta} .$$

(B5)

APPENDIX C: RENORMALIZATION OF CORRELATION FUNCTIONS IN THE WEAK-COUPLING REGIME

In this appendix, we give the details of the derivation for the renormalization of the exponents of the correlation functions in the weak-coupling regime.

The Green's function

$$G_{\psi\psi}(\tau) = -\langle T\psi(\tau)\psi^\dagger(0) \rangle ,$$

(C1)

where $\psi^\dagger = (d^\dagger, c^\dagger)$, can be expanded in terms of the flipping part of the Hamiltonian H_f,

$$G_{\psi\psi}(\tau) = -\frac{1}{Z} \int DcDdT \left\{ \psi(\tau)\psi^\dagger(0)\exp\left[-\left[S_0 + \int_0^\beta d\tau H_f(\tau) \right] \right] \right\}$$

$$= \frac{1}{Z} \sum_{n=0}^\infty \int_{\xi_0}^{\beta-\xi_0} d\tau_n \cdots \int_{\xi_0}^{\tau_{i+1}-\xi_0} d\tau_i \cdots \int_{\xi_0}^{\tau_2-\xi_0} d\tau_1 A(\alpha;\tau;0;\tau_n,\ldots,\tau_1) ,$$

(C2)

where the transition amplitude

$$A(\alpha;\tau;0;\tau_n,\ldots,\tau_1) = (-1)^n \int DcDd \langle \alpha | T[\exp(-\beta H_0)\psi(\tau)H_f(\tau_n) \cdots H_f(\tau_i) \cdots H_f(\tau_1)\psi^\dagger(0)] | \alpha \rangle .$$

(C3)

Without loss of generality, we take $\tau > 0$. For a given history similar to that illustrated in Fig. 1, the external time τ lies between two flips, say $\tau_{k-1} < \tau < \tau_k$. The transition amplitude has the following form once a complete set of local states is inserted at every discrete time

$$A(\alpha;\tau;0;\tau_n,\ldots,\tau_1) = (-1)^n \sum_{\alpha_1,\ldots,\alpha_n} \int Dc \exp[-H_\alpha(\beta-\tau_n)]Q(\alpha,\alpha_n) \cdots$$

$$\times \exp[-H_{\alpha_{k+1}}(\tau_{k+1}-\tau_k)]Q(\alpha_{k+1},\alpha_m)\exp[-H_{\alpha_m}(\tau_k-\tau)]$$

$$\times \psi \exp[-H_{\alpha_m}(\tau-\tau_{k-1})]Q(\alpha_{m'},\alpha_{k-1})\exp[-H_{\alpha_{k-1}}(\tau_{k-1}-\tau_{k-2})] \cdots$$

$$\times \exp[-H_{\alpha_2}(\tau_2-\tau_1)]Q(\alpha_2,\alpha_1)\exp[-H_{\alpha_1}\tau_1]\psi^\dagger ,$$

(C4)

where $|\alpha_m\rangle$ and $|\alpha_{m'}\rangle$ label states after and before the external time τ. The operator $\psi^\dagger$, on the other hand, flips from the local state $|\alpha\rangle$ to $|\alpha_1\rangle$. We emphasize that the external fermion operators place constraints on the hopping history of the impurity: the insertion of a d electron creates a charge kink, while the insertion of a local c electron does not create any kink.

Tracing out the conduction electron degrees of freedom,

$$A(\alpha;\tau;0;\tau_n,\ldots,\tau_1)=Z_c\sum_{\alpha_{n+1}=\alpha,\alpha_1,\ldots,\alpha_n} y'_{\alpha_{n+1},\alpha_n}\cdots y'_{\alpha_{k+1},\alpha_m}y'_{\alpha_{m'},\alpha_{k-1}}\cdots y'_{\alpha_2,\alpha_1}$$

$$\times\exp\left[E'_\alpha\tau_n-E'_{\alpha_1}\tau-\sum_{i=2}^{n-1}E'_{\alpha_{i+1}}(\tau_{i+1}-\tau_i)\right]\langle O(\alpha_{n+1},\alpha_n)(\tau_n)\cdots O(\alpha_{k+1},\alpha_m)(\tau_k)$$

$$\times\Psi_{\alpha_m,\alpha_{m'}}(\tau)O(\alpha_{m'},\alpha_{k-1})(\tau_{k-1})\cdots O(\alpha_2,\alpha_1)(\tau_1)\Psi^\dagger_{\alpha_1,\alpha}(0)\rangle\ , \tag{C5}$$

where $\Psi^\dagger_{\alpha,\beta}=(D^\dagger_{\alpha,\beta},C^\dagger_{\alpha,\beta})$ have the following form:

$$(D_\sigma)_{\alpha,\beta}(\tau)\equiv\exp[ie^\gamma_D\Phi_\gamma(\tau)]\delta_{\alpha,|0\rangle}\delta_{\beta,|\sigma\rangle}\ ,$$
$$(C_\sigma)_{\alpha,\beta}(\tau)\equiv\exp[ie^\gamma_C\Phi_\gamma(\tau)]\delta_{\alpha,\beta}\ , \tag{C6}$$

with

$$e^\gamma_D=\frac{\delta_1}{\pi}+\frac{\delta_2}{\pi}\delta_{\gamma,\sigma}\ ,$$
$$e^\gamma_C=-\delta_{\gamma,\sigma}\ . \tag{C7}$$

The transition amplitude now has again a simple form in boson representation through

$$\langle O(\alpha_{n+1},\alpha_n)(\tau_n)\cdots O(\alpha_{k+1},\alpha_m)(\tau_k)\Psi_\sigma(\tau)O(\alpha_{m'},\alpha_{k-1})(\tau_{k-1})\cdots O(\alpha_2,\alpha_1)(\tau_1)\Psi^\dagger_\sigma(0)\rangle$$

$$=\int\exp\left[-S_c+\int_0^\beta D\tau'\sum_\gamma j_\gamma(\tau')\Phi_\gamma(\tau')\right]\ , \tag{C8}$$

where

$$j_\gamma(\tau')=\sum_{i=1}^n{}'\delta(\tau'-\tau_i)e^\gamma_{\alpha_{i+1},\alpha_i}+\delta(\tau'-\tau_{k-1})e^\gamma_{\alpha_{m'},\alpha_{k-1}}+\delta(\tau'-\tau_k)e^\gamma_{\alpha_k,\alpha_m}$$

$$+\delta(\tau'-\tau_1)e^\gamma_{\alpha_1,\alpha_2}+\delta(\tau'-\tau_n)e^\gamma_{\alpha_n,\alpha}+\delta(\tau'-\tau)e^\gamma_\Psi+\delta(\tau')e^\gamma_{\Psi^\dagger}\ . \tag{C9}$$

Here a primed sum means a summation, which excludes $n,1,k-1,k$. Therefore,

$$\langle O(\alpha_{n+1},\alpha_n)(\tau_n)\cdots O(\alpha_{k+1},\alpha_m)(\tau_k)\Psi_\sigma(\tau)O(\alpha_{m'},\alpha_{k-1})(\tau_{k-1})\cdots O(\alpha_2,\alpha_1)(\tau_1)\Psi^\dagger_\sigma(0)\rangle=\exp\left[-\sum_\gamma A^\gamma\right]\ , \tag{C10}$$

where

$$A^\gamma=\frac{1}{2}\sum_{i_1}{}'\sum_{i_2}{}'e_{\alpha_{i_1+1},\alpha_{i_1}}^\gamma\,e^\gamma_{\alpha_{i_2+1},\alpha_{i_2}}\ln\frac{|\tau_{i_1}-\tau_{i_2}|}{\xi_0}+\frac{1}{2}\sum_{i_1}{}''\sum_{i_2}{}''e^\gamma_{\alpha_{i_1+1},\alpha_{i_1}}e^\gamma_{\alpha_{i_2+1},\alpha_{i_2}}\ln\frac{|\tau_{i_1}-\tau_{i_2}|}{\xi_0}$$

$$+\sum_{i_2}{}'\sum_{i_2}{}''e^\gamma_{\alpha_{i_1+1},\alpha_{i_1}}e^\gamma_{\alpha_{i_2+1},\alpha_{i_2}}\ln\frac{|\tau_{i_1}-\tau_{i_2}|}{\xi_0}+\sum_i{}'e^\gamma_{\alpha_{i+1},\alpha_i}e^\gamma_\Psi\ln\frac{\tau_i}{\xi_0}+\sum_i{}'e^\gamma_{\alpha_{i+1},\alpha_i}e^\gamma_\Psi\ln\frac{|\tau_i-\tau|}{\xi_0}+e^\gamma_\Psi e^\gamma_\Psi\ln\frac{\tau}{\xi_0}$$

$$+\sum_i{}'h_i(\tau_{i+1}-\tau_i)+h_m(\tau_k-\tau)+h_{m'}(\tau-\tau_{k-1})+h_\alpha(\beta-\tau_n)+h_{\alpha_1}\tau_1\ . \tag{C11}$$

Here the double-primed summation extends over the neighbors of the 0 and τ, which include $\tau_n,\tau_1,\tau_{k-1},\tau_k$.

We are now ready to perform the RG calculation, by integrating out degrees of freedom in the range $(\xi,\xi+d\xi)$. This again leads to renormalization contributions of three kinds: (a) simple rescaling, (b) integrating out non-neutral pairs, and (c) integrating neutral pairs. The contributions from simple rescaling of the cutoff, as well as from integrating out the primed kink pairs, give rise to scaling of the fugacities, stiffness constants and the fields,

which are the same as those in the partition function.

On the other hand, integrating out the pairs formed between a doubly primed kink and its neighbor in the primed kinks will contribute directly to the renormalization of the correlation functions. For the Green's functions, there are four terms contributing to the renormalization of the propagators. Contributions from the pair of kinks before and after the external time τ cancel unless the original states before and after τ are different. Collecting all these contributions, we arrive at the results

$$\frac{d(\alpha_{dd}\ln(\tau/\xi))}{d\ln\xi} = -2\sum_m \sum_\gamma (e_D^m e_{\alpha_m,\gamma}^m \gamma_{\alpha_m,\gamma}^2 + e_D^m e_{\alpha_{m'},\gamma}^m \gamma_{\alpha_{m'},\gamma}^2)\ln\frac{\tau}{\xi} ,$$

$$\frac{d(\alpha_{cd}\ln(\tau/\xi))}{d\ln\xi} = \sum_m \sum_\lambda \sum_\gamma e_{\lambda,\lambda}^m (e_{\alpha_m,\gamma}^m y_{\alpha_m,\gamma}^2 - e_{\alpha_{m'},\gamma}^m y_{\alpha_{m'},\gamma}^2)\ln\frac{\tau}{\xi} ,$$

$$\frac{d(\alpha_{cc}\ln(\tau/\xi))}{d\ln\xi} = 0 ,$$

(C12)

where $\alpha_{dd}, \alpha_{cc}, \alpha_{dc}$ are the exponents for G_{dd}, G_{cc}, G_{dc}, respectively, in the algebraic dependence on imaginary time. Integrating from $\xi = \xi_0$ and $\xi = \tau$ gives rise to the correction to the Green's function due to the fugacities.

The two-particle correlation functions can be calculated following the same procedure. The results are given in Sec. V A.

[1]P. W. Anderson, Physica C **185-189**, 11 (1991); P. W. Anderson and R. Schrieffer, Phys. Today, **44** (6), 54 (1991), and references therein.

[2]A. Ruckenstein and C. Varma, Physica C **185-189**, 134 (1991).

[3]V. J. Emery, in *Highly Conducting One-Dimensional Solids*, edited by J. T. Devreese *et al.* (Plenum, New York, 1979); J. Solyom, Adv. Phys. **28**, 201 (1979).

[4]F. D. M. Haldane, J. Phys. C **14**, 2585 (1981).

[5]A. Sudbo, C. M. Varma, T. Giamarchi, E. B. Stechel, and R. T. Scalettar, Phys. Rev. Lett. **70**, 978 (1993).

[6]R. Shankar (unpublished).

[7]For a recent review see D. Vollhardt, in *Correlated Electron Systems*, edited by V. J. Emery (World Scientific, Singapore, in press).

[8]A. Georges and G. Kotliar, Phys. Rev. B **45**, 6479 (1992).

[9]A. Georges, G. Kotliar, and Q. Si, Int. J. Mod. Phys. B **6**, 705 (1992).

[10]M. J. Rozenberg, X. Y. Zhang, and G. Kotliar, Phys. Rev. Lett. **69**, 1236 (1992); X. Y. Zhang, M. J. Rozenberg, and G. Kotliar, *ibid.* **70**, 1666 (1993).

[11]A. Georges and W. Krauth, Phys. Rev. Lett. **69**, 1240 (1992).

[12]M. Jarrell, Phys. Rev. Lett. **69**, 168 (1992).

[13]F. D. M. Haldane, Phys. Rev. Lett. **40**, 416 (1978); Ph.D. thesis, University, of Cambridge, 1977 (unpublished); J. Phys. C **11**, 5015 (1978).

[14]A. J. Leggett, S. Chakravarty, A. T. Dorsey, M. P. A. Fisher, and W. Zwerger, Rev. Mod. Phys. **59**, 1 (1987).

[15]P. B. Wiegmann and A. M. Finkelstein, Zh. Eksp. Teor. Fiz. **75**, 204 (1978) [Sov. Phys. JETP **48**, 102 (1978)].

[16]P. Schlottmann, Phys. Rev. B **25**, 4815 (1982), and references therein.

[17]F. Guinea, V. Hakim, and A. Muramatsu, Phys. Rev. B **32**, 4410 (1985).

[18]T. Giamarchi, C. Varma, A. Ruckenstein, and P. Nozieres, Phys. Rev. Lett. **70**, 3967 (1992); C. M. Varma and T. Giamarchi, in *Strongly Interacting Fermions and High T_c Superconductivity*, edited by B. Doucot (North-Holland, Amsterdam, in press).

[19]I. Perakis, C. Varma, and A. Ruckenstein, Phys. Rev. Lett. **70**, 3467 (1993).

[20]F. D. M. Haldane, Phys. Rev. B **15**, 281 (1977); **15**, 2477 (1977).

[21]J. L. Cardy, J. Phys. A **14**, 1407 (1981); see also S. Chakravarty and J. Hirsch, Phys. Rev. B **25**, 3273 (1982).

[22]Q. Si and G. Kotliar, Phys. Rev. Lett. **70**, 3143 (1993).

[23]U. Brandt and C. Mielsch, Z. Phys. B **75**, 365 (1989); **79**, 295 (1990).

[24]V. Janis, Z. Phys. B **83**, 227 (1991).

[25]P. Lloyd, J. Phys. C **2**, 1717 (1969); M. Acquarone, D. Tay, and J. Spalek, J. Phys. C **15**, 959 (1982).

[26]Q. Si, G. Kotliar, and A. Georges, Phys. Rev. B **46**, 1261 (1992).

[27]C. M. Varma, Rev. Mod. Phys. **48**, 219 (1976); D. Khomskii, Usp. Fiz. Nauk **129**, 443 (1979) [Sov. Phys. Usp. **22**, 879 (1979)].

[28]V. Emery, Phys. Rev. Lett. **58**, 2794 (1987).

[29]C. M. Varma, S. Schmitt-Rink, and E. Abrahams, Solid State Commun. **62**, 681 (1987).

[30]P. W. Anderson, G. Yuval, and D. R. Hamman, Phys. Rev. B **1**, 4464 (1970); P. W. Anderson and G. Yuval, Phys. Rev. Lett. **23**, 89 (1969); P. W. Anderson, J. Phys. C **3**, 2436 (1970).

[31]K. G. Wilson, Rev. Mod. Phys. **47**, 773 (1975).

[32]J. M. Kosterlitz and D. J. Thouless, J. Phys. C **6**, 1181 (1973); J. M. Kosterlitz, J. Phys. C **7**, 1046 (1974).

[33]G. D. Mahan, Phys. Rev. **163**, 612 (1967); M. Combescot and P. Nozières, J. Phys. (Paris) **32**, 913 (1971); P. W. Anderson, Phys. Rev. Lett. **18**, 1049 (1967); J. J. Hopfield, Commun. Solid State Phys. **2**, 40 (1969).

[34]H. R. Krishnamurthy, K. G. Wilson, and J. W. Wilkins, Phys. Rev. B **21**, 1044 (1980).

[35]It resembles the hexatic phase in the two-dimensional melting within which, unbinding occurs for dislocations but not for disclinations. For a review see D. Nelson, in *Phase Transitions and Critical Phenomena*, edited by C. Domb and J. L. Lebowitz (Academic, London, 1983), Vol. 7, p. 1.

[36]A. A. Abrikosov and A. A. Migdal, J. Low Temp. Phys. **3**, 519 (1970); M. Fowler and A. Zawadowski, Solid State Commun. **9**, 471 (1971).

[37]G. Kotliar, Ph.D. thesis, Princeton University, 1983 (unpublished).

[38]The finite-U problem can be dealt with through the scaling equations in a finite field given in Appendix B.

[39]K. D. Schotte and U. Schotte, Phys. Rev. **182**, 479 (1969).

[40]The $(-1)^n$ factor is absorbed by the ordering of the conduction electron operators in the corresponding correlation function.

[41]At finite temperature $T=1/\beta$, $1/\tau$ is replaced by $(\pi/\beta)/\sin[(\pi/\beta)\tau]$.

[42]Because of rotational invariance in spin space the second and the fourth equations should be identical. This is achieved explicitly by expanding to quadratic order in the small quantities $y_j = (1 - \epsilon_j)/2$.

[43]P. Coleman, Phys. Rev. B **29**, 3035 (1984); N. Read and D. M. Newns, J. Phys. C **16**, 3273 (1983); A. Auerbach and K.

Levin, Phys. Rev. Lett. **57**, 877 (1986); A. J. Millis and P. A. Lee, Phys. Rev. B **35**, 3394 (1987).

[44]M. Grilli, R. Raimondi, C. Castellani, C. Di Castro, and G. Kotliar, Phys. Rev. Lett. **66**, 1236 (1990).

[45]P. G. J. van Dongen, Phys. Rev. B **45**, 2267 (1992).

[46]For large values of the hybridization, d and c electrons are expected to be bound together. Self-consistency again gives rise to a finite density of states of the electron bath; Q. Si, M. Rozenberg, and G. Kotliar (unpublished).

[47]N. Furukawa and M. Imada, J. Phys. Soc. Jpn. **60**, 3604 (1991); **61**, 3331 (1992).

[48]For a review see Q. Si, Int. J. Mod. Phys. B (to be published).

[49]P. W. Anderson and Z. Zou, Phys. Rev. Lett. **60**, 132 (1988); L. B. Ioffe and A. Larkin, Phys. Rev. B **39**, 8988 (1989); N. Nagaosa and P. A. Lee, Phys. Rev. Lett. **64**, 2450 (1990); L. B. Ioffe and G. Kotliar, Phys. Rev. B **42**, 10 348 (1990).

[50]G. Kotliar and Q. Si, in *Proceedings of the Meeting of the European Physical Society, Regensburg, Germany, 1993* [Phys. Scr. (to be published)].